Chapter 3.1

Cell Membrane Mechanics and Adhesion

3.1.1 Introduction

Membranes perform a critical function, providing a selective barrier between the cell interior and the living processes inside, and the lifeless, often inhospitable environment outside. In the simplest of terms, the cell membrane can be thought of as a lipid bilayer that separates the cytoplasmic and extracellular domains. Indeed, our approach to modeling membrane mechanics relies much on this simplification. The true cell membrane, however, is vastly more complex than this simple representation would suggest, and we begin this chapter by describing some of this complexity and its implications to the mechanical properties of the cell. Since the membrane and associated structures behave as an integral structural element of the cell, we next develop the methods for investigating membrane mechanics, both theoretical and experimental. In the last section of this chapter, the means by which the cell adheres to its environment are discussed along with the methods used to probe these adhesive properties through experimentation and analyze the results quantitatively.

3.1.2 Membrane Structure and Biology

Membrane composition and organization

Although much of the discussion of this chapter will be directed to the outer, limiting cell membrane, it is important to realize that much of the membrane of a cell is intracellular and serves the purpose of partitioning regions in the cell, such as the nucleus or mitochondria, from the cytoplasm. While each type of membrane has its own unique characteristics, their basic

structure remains much the same. For that reason, despite our focus on the outer or *plasma membrane*, the material in this chapter applies more generally to all cell-associated membranes.

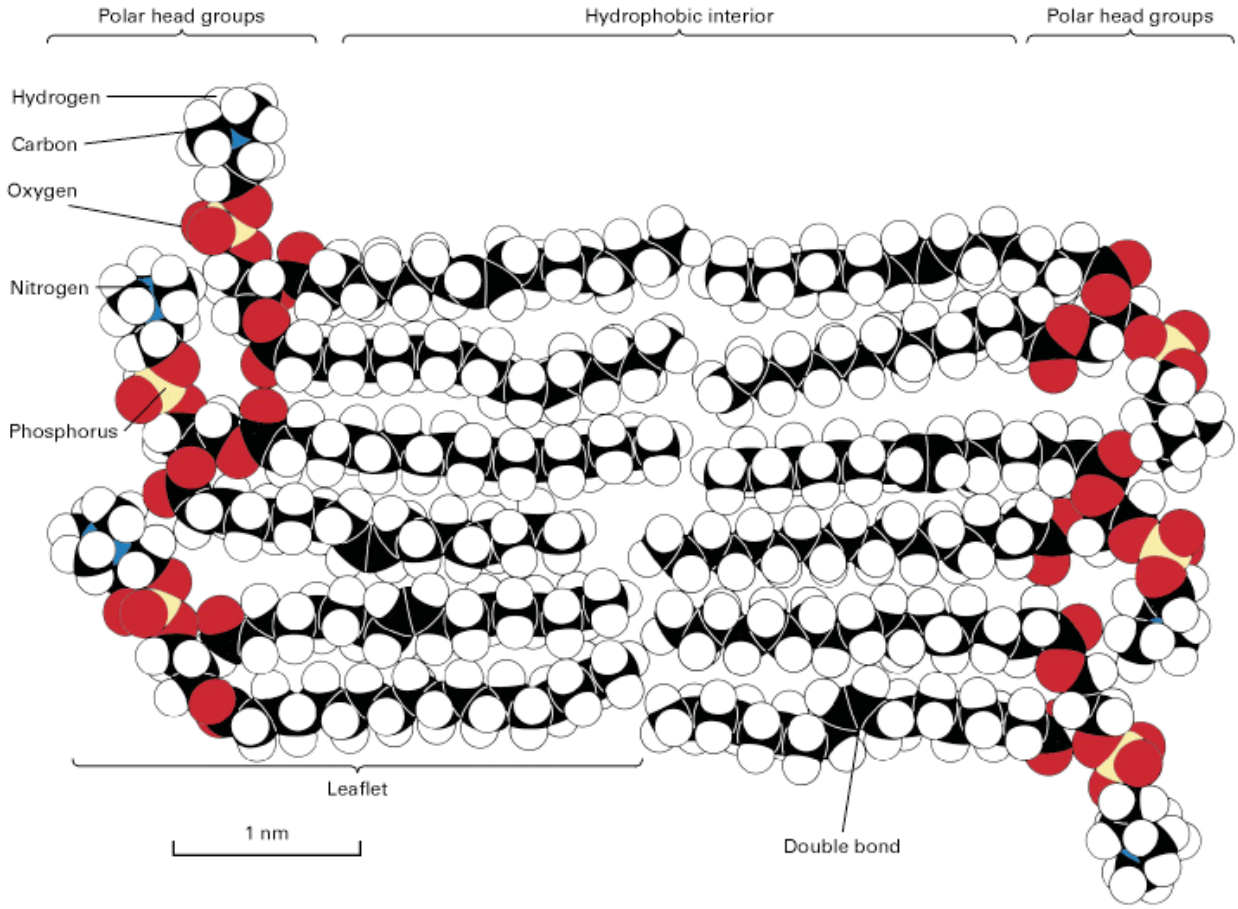

Fig. 3.1.1. A space-filling model of the lipid bilayer showing the hydrophilic heads (polar head groups) on the outside, and the hydrophobic tails pointing in, on the interior. The total thickness of the bilayer is about 6 nm. [Reproduced from *Molecular Cell Biology*, Lodish, et al., 2000]

When we use the term *membrane*, we are generally referring to the phospholipid bilayer and the proteins associated with it. The phospholipids contained in the membrane are arranged in two layers or *leaflets*, with their hydrophobic tails pointing inward and their hydrophilic heads outward. Together, they constitute a bilayer about 6 nm in thickness (Fig. 3.1.1). Four phospholipids account for more than half the lipid in most membranes; these are phosphatidylcholine, sphingomyelin, phosphatidylserine, and phosphatidylethanolamine. The first and second of these are predominantly in the outer leaflet while the third and fourth are more common in the inner leaflet. In addition to these phospholipids, the membrane contains glycolipids and cholesterol. While the amount of glycolipid is small, constituting only about 2%

of the total lipid content, cholesterol is a major membrane constituent, roughly 20% by weight, a value that remains quite constant among the different cell types.

Several of these lipids are critical for their role in determining membrane structural integrity. These include the four major phospholipids and cholesterol. For example, both the bending stiffness and the viscosity of the lipid bilayer, sometimes referred to as *membrane fluidity*, are strongly dependent on the cholesterol content.

Other important membrane constituents are the membrane-associated proteins, which account for roughly 50% of the membrane by weight but because of their relatively large molecular weight, only about 1-2% of the number of molecules comprising the membrane. These serve a variety of functions from signaling, to the transport of ions and other molecules across the membrane, to the adhesion of the cell to surrounding structures as will be discussed more later. One subclass includes the *integral membrane proteins*, those that penetrate into the lipid bilayer, can be classified according to their means of attachment to the bilayer:

- proteins that attach primarily through interactions with the hydrophobic core (this subgroup contains most ion channels),
- transmembrane proteins attached by only one hydrophobic segment (including many membrane-bound antibodies, some receptors of the integrin family, and several other types of receptor),
- proteins attached to the membrane by lipid anchors, or
- proteins adsorbed to the membrane through interactions with the charged head groups.

Some membrane-associated proteins are bound through other proteins (Fig. 3.1.2); these are called *peripheral proteins* and can be made to dissociate from the membrane by introducing fluids with extreme values of pH or high salt concentrations that disrupt the covalent bonds typically used for attachment.

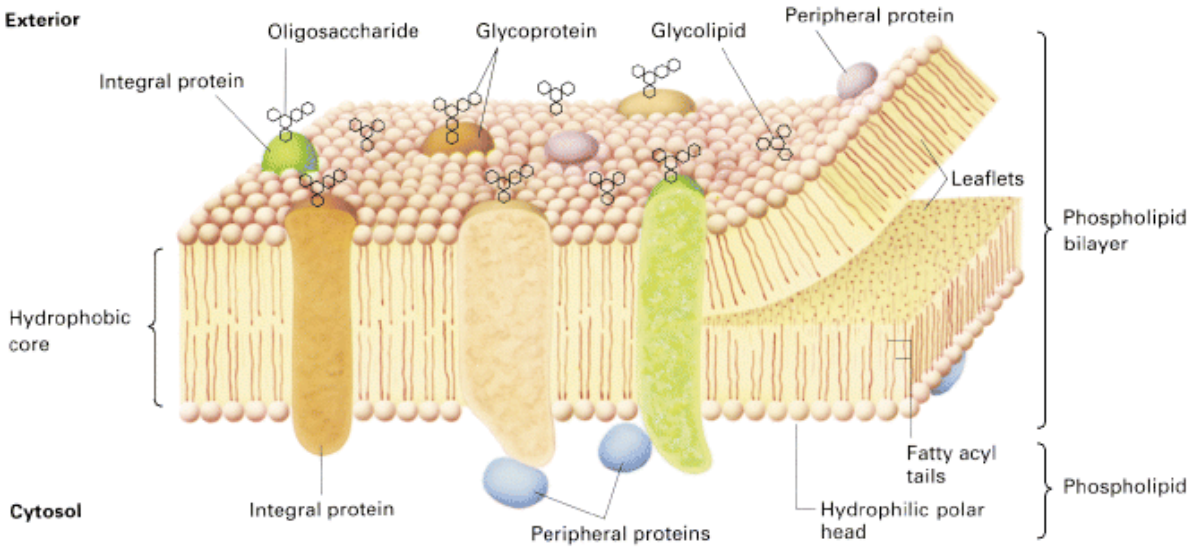

Fig. 3.1.2. Schematic of the lipid bilayer and associated proteins, either integral or peripheral. [Reproduced from Molecular Cell Biology, Lodish, et al., 2000]

The critical importance of these proteins can be illustrated by describing some of their many functions. One group of proteins serves as ion or water channels and pumps to control the intracellular ionic concentrations (H^+, Na^+, Cl^+, Mg^{++}, Ca^{++}). In the case of the red blood cell or *erythrocyte*, for example, the cytosol is maintained at a potential approximately -6 mV relative to the blood plasma. Intracellular osmotic pressure (~150 mosm) and pH (~7.4) are also maintained within narrow limits. Many channels are active ion transporters, pumping ions against a concentration gradient and requiring an external source of energy, often by ATP hydrolysis. Others, however, perform *facilitated diffusion*, meaning that they help to regulate the exchange of ions across the membrane in the direction of the concentration gradient, but require no external energy. One class of these of particular interest in biomechanics includes the mechanically-sensitive ion channels that open or close under the action of stresses transmitted by the membrane or via attachments to the cytoskeleton or extracellular matrix. One such channel located in the stereocilia of hair cells in the tympanic membrane mediates the sensation of sound. The mechanism by which forces regulate these channels is discussed in Chapter 3.3. Other ion channels are regulated by a change in protein conformation resulting from binding by some signaling molecule (so-called *ligand-gated channels*), or by changes in the transmembrane voltage potential (*voltage-gated channels*). Much of what we know about these ion channels comes from experiments using the *patch clamp technique*, in which drawing it into the tip of a micropipet isolates a small section of membrane. This method, developed by Neher and

Sakmann in 1976, has spawned many of the experiments on which our current understanding of membrane ion transport is based.

Other integral membrane proteins are used for adhesion of the cell to surrounding structures, for signaling, or for the control of biochemical reactions. Discussion of adhesion proteins will come later, in Section 3.1.6. Signaling is accomplished in a variety of ways, but is most often mediated by the transfer of molecules across the membrane either directly by diffusion or via selective channels, or by binding of a ligand to a cell surface receptor. Each time a signal is "received" by means of receptor-ligand binding, the result is a conformational change in the receptor that initiates other biological processes via a *signaling cascade* involving a host of other intermediate molecules. Not infrequently, the reaction initiated by ligand-receptor binding is with another protein located within the membrane or closely associated with it. Being constrained to two dimensions, rather than free to move in three, can greatly accelerate reactions that are diffusion-limited. For example, the time required for a molecule to reach a target of diameter d_T located a distance L away is approximately $L^3/(3Dd_T)$ in three dimensions and $(L^2/2D)\ln(L/d_T)$ in two, where D is the diffusion coefficient (Hardt 1979).

Recognizing its fluid-like nature and multi-component structure, Singer and Nicolson proposed the *fluid mosaic model* for the membrane in 1972. This model emphasizes that the lipids form a highly fluid-like phase while the proteins tend to aggregate in isolated islands that are relatively rigidly structured, giving rise to a mosaic-like arrangement. Both the proteins and lipids are free to diffuse within the plane of the membrane unless tethered to fixed structures either internal or external to the cell. The fluid-like nature of the membrane, especially the lipid portion, accounts for the low resistance to shear deformations in the plane of the membrane. In addition, the hydrophobic interior behaves essentially like a hydrocarbon fluid allowing the two leaflets to slide freely relative to one another.

Aside from the lipid bilayer, the cell plasma membrane has associated macromolecular structures on both intra- and extracellular sides giving rise to a three-layer composite construction. On the intracellular side, the membrane is physically attached to a cortex or the cytoskeleton. The cortex is a dense, filamentous structure that lends stiffness to the membrane, and can also interact with various transmembrane proteins, often impeding their free diffusion either by steric interactions or direct chemical bonding. In some cells, the cortex is simply a region of dense cytoskeletal matrix in the vicinity of the bilayer. In others, it exhibits a distinctly different structure or composition. For example, erythrocytes possess a cortex comprised of a network of spectrin tetramers linked by actin filaments. This network is attached to the membrane by ankyrin and the integral membrane protein band 3 (Fig. 3.1.3). This spectrin network accounts for much of the bending stiffness exhibited by the red cell membrane.

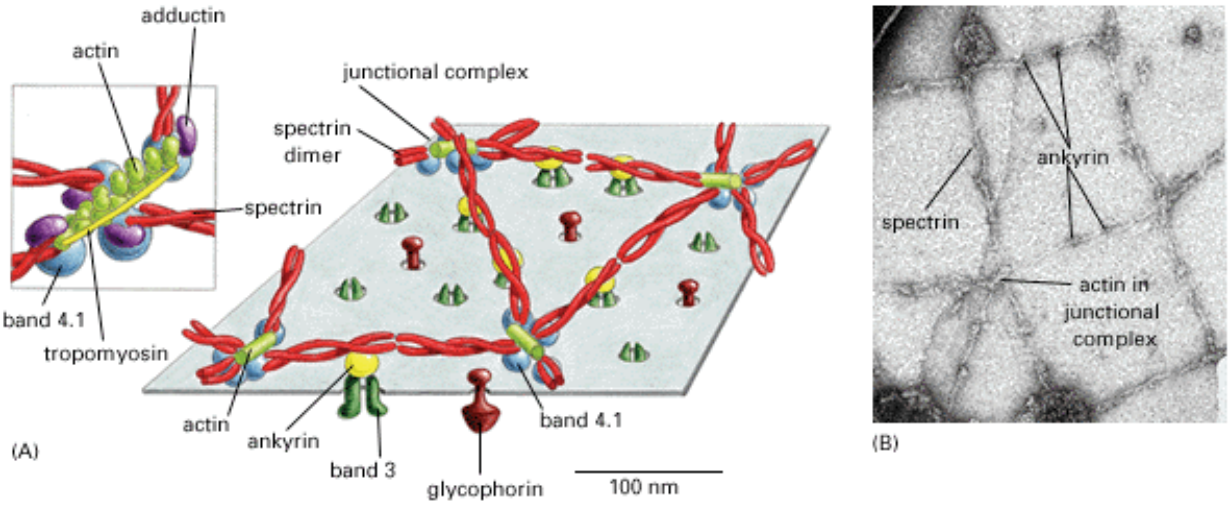

Fig. 3.1.3. Structure of the membrane-associated cortex in an erythrocyte as viewed from the inside of the cell. a) Schematic representation showing the arrangement of the spectrin filaments joined by short segments (13 monomers) of actin and tethered to the membrane through ankyrin and band 3. Junctional complexes containing actin, tropomyosin, adductin and band 4.1 also bind to band 3 and glycophorin. b) An electron micrograph showing the same structures. [From Molecular Biology of the Cell, Bruce Alberts, Dennis Bray, Julian Lewis, Martin Raff, Keith Roberts, James D. Watson © 1994]

External to most cells is found a *glycocalyx*, which has been shown to extend as far as 0.5 μm from the surface of endothelial cells where it forms a compressible barrier separating circulating erythrocytes and leucocytes from the endothelial membrane. The glycocalyx is comprised of short oligosaccharide chains, glycoproteins, glycolipids and high molecular weight proteoglycans, all organized into an interconnected network with an overall negative charge. Although its function is not completely understood, it apparently plays a role in macromolecular transport across the endothelium and is an important factor in the interaction between blood-borne cells and the endothelium. Studies have demonstrated that the glycocalyx in a capillary is readily compressed by a passing leukocyte, yet is sufficiently rigid to prevent flowing erythrocytes from approaching the endothelial surface (Fig. 3.1.4).

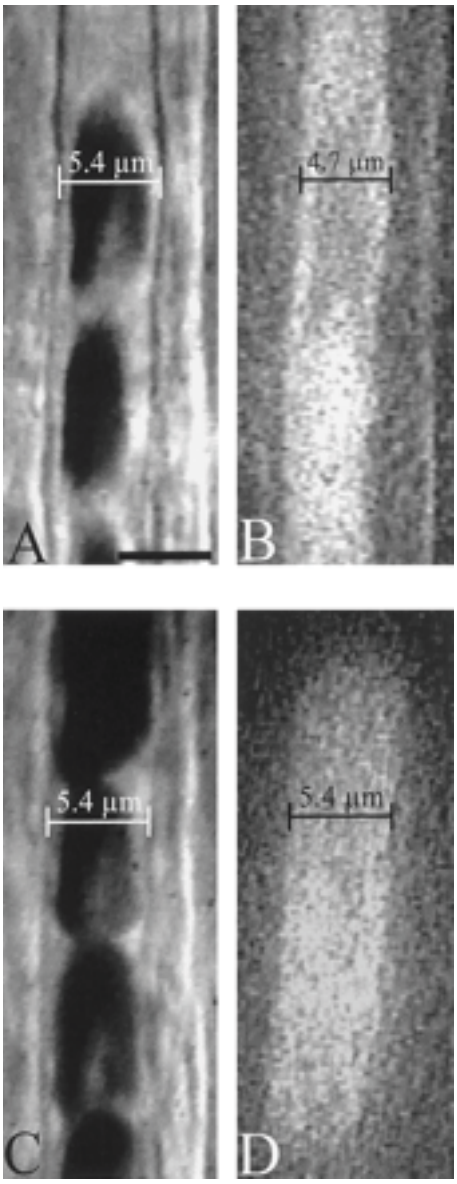

Fig. 2.1.4. Images of a capillary segment in the hamster cremaster muscle with an intact glycocalyx (A,B) and with the glycocalyx collapsed by treatment of the vessel with epi-illumination (C,D), using either bright field illumination (A,C) or fluorescent imaging using a dye too large to penetrate the glycocalyx (70 kD molecular weight FITC-dextran). The capillary wall is visualized by a membrane-specific dye, PKH26 in A and C. Width of the glycocalyx is indicated by the gap between the erythrocytes and the wall in A and C, and by the change in effective capillary diameter before (B) and after (D) epi-illumination. In this series, capillary diameter increased from 4.7 to 5.4 μm suggesting a width of the glycocalyx of 0.35 μm. [Reproduced from Vink & Duling (Vink and Duling 1996).

3.1.3 Membrane Mechanics

For the purpose of analysis, we treat the cell membrane as a homogeneous two-dimensional plate or sheet completely enclosing the cytoplasm. The membrane referred to here can be thought of either as the lipid bilayer by itself, or more typically, as the bilayer plus the associated cortex of cytoskeletal filaments and glycocalyx on the extracellular surface. In addition, though not explicitly recognized in the analysis, transmembrane proteins and their attachments to the intracellular and extracellular milieu are included in terms of their influence on the continuum

properties of the model. Were it not for these, the membrane would exhibit little resistance to shear deformation.

In qualitative terms, the lipid bilayer can be thought of as a two-dimensional fluid, within which the individual lipid molecules, or other molecules embedded in the membrane, are relatively free to move about by diffusion or directed motion. Phospholipid molecules in either of the two layers resist being pulled apart, however, so each layer is highly inextensible. This also contributes to the bending stiffness, which is low in absolute terms, but high for such a thin layer, since bending requires one layer to expand while the other is compressed. By contrast, the two layers readily slide relative to each other. These qualitative notions are put in more quantitative terms in the next section.

Types of deformation

Any deformation can be thought of, in general terms, as a superposition of several simpler deformations. For small strains in which linearization is appropriate, the principle of superposition is rigorously valid. For larger strains, however, linear theory breaks down and superposition can only be used as a rough, qualitative guide in visualizing combined influences. Here we present the three primary types of deformation: pure extension, pure bending, and pure shear. Later, we also consider the influence of membrane viscosity in time-dependent deformations.

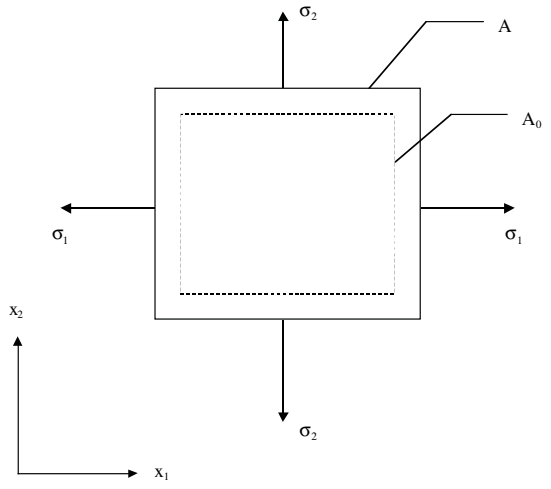

Fig. 3.1.5. A membrane, initially of area A_0, subjected to a uniform extensional stress along its edges, $\sigma_1 = \sigma_2$, causing an increase in area to A.

Pure extension. In discussing the extensional stiffness of the membrane, we need to distinguish the behavior at low tension from that at high tension. As you first begin to apply an extensional

stress at the edges of a lipid bilayer, the projected or *apparent* membrane area first increases while the actual or true membrane area remains constant. This results from the suppression of out-of-plane undulations. Forces acting to resist membrane flattening originate from entropic effects analogous to those seen in the case of a flexible polymer as its end-to-end distance is increased – many more membrane configurations exist with undulations compared to the single perfectly flat state. Only when these undulations have been eliminated does the *true* membrane area, proportional to the surface area per molecule group, begin to increase, and this is associated with a relatively abrupt increase in extensional stiffness. For now, we consider only the stiffness of a flat membrane and leave the discussion of undulations of entropic origin to a later point in the chapter. Hence we initially neglect all entropic effects, or equivalently, consider the membrane to be at zero temperature.

Based in this assumption, consider an infinitesimal plate, initially of area $A_0 = L_0^2$ that is deformed by a uniform normal stress $\tau_{11} = \sigma_1 = \tau_{22} = \sigma_2$ applied to its edges (Fig. 3.1.5) to a new area, A. Previously, we derived the expressions relating stress and strain, which in two dimensions and in the absence of stresses normal to the x_1-x_2 plane, can be written:

$$\sigma_\alpha = \frac{E}{1-\nu^2}\left(\varepsilon_\alpha + \nu\varepsilon_\beta\right) \tag{2.1}$$

where the length of one edge, $L_\alpha = L_0(1+\varepsilon_\alpha)$. Note that in this chapter, we use the subscripts α, β rather than i, j to distinguish stresses and strains in two dimensions from those, more generally, in three. Thus, whereas i and j can be either 1, 2 or 3, α and β are restricted to being either 1 or 2. When this stress is uniform in the plane of the membrane (the x_1- x_2 plane) it can be replaced, without loss of generality, by a surface tension N_α (force per unit length) defined as $\sigma_\alpha \cdot h$ where h is the thickness of the membrane. These can be combined in the case when $N_1 = N_2 = constant$ and, consequently, $\varepsilon_1 = \varepsilon_2 = \varepsilon$ to give:

$$N = \frac{Eh}{1-\nu}\varepsilon \tag{2.2}$$

In terms of a plate stretched uniformly in both directions, we can define the areal strain as:

$$\frac{\Delta A}{A_0} = \frac{A - A_0}{A_0} = \frac{L_0^2(1+\varepsilon)^2 - L_0^2}{L_0^2} \cong 2\varepsilon \tag{2.3}$$

where the last approximation is appropriate for small strains. By combining this result with eqn. (2.2), we can define the *area expansion modulus,* K_e (units of N/m),

$$N = \frac{Eh}{2(1-\nu)}\frac{\Delta A}{A_0} \equiv K_e \frac{\Delta A}{A_0} \tag{2.4}$$

Note that although we used the continuum structural equations in our analysis, the final result can also be viewed as simply the definition of the area expansion modulus and applies regardless of whether or not the membrane can be modeled as a continuum.

Experimental measurements of K_e lie in the range of 0.1-1 N/m for various types of lipid bilayers and about 0.45 N/m (450 dyn/cm) for red blood cell membranes (Waugh and Evans 1979). These numbers suggest that cell membranes are quite resistant to extension and, for that reason, are often treated as inextensible[1]. This high resistance to area change is in large part due to the energy penalty associated with exposing the hydrophobic core of the membrane to water that occurs as the spacing between individual amphiphilic molecules is increased [for a detailed description of bilayer structure and thermodynamics, see Tanford (1980), or Israelachivili (1991)]. Continuing to increase extensional stress, the lipid bilayer eventually ruptures, but at very small extensional strains, in the vicinity of 2 to 3% (Mohandas & Evans, 1990). Note that a bilayer in a lipid vescicle, for example, stretches primarily by increasing the area per molecule since recruitment of additional material to the membrane occurs very slowly.

Using these expressions, we can estimate the level of surface tension at which the membrane would rupture. At a 3% extensional strain (6% areal strain) uniformly applied in the x_1-x_2 plane, the surface tension at rupture would be about 0.06 N/m if we use a value near the higher end of the observed range, K_e = 1 N/m. Using Laplace's law [see eqn. (2.27)] for the relationship between the pressure difference (ΔP) across a spherical shell of radius $R = 1\ \mu m$ and the surface tension in the shell gives us:

$$\Delta P = \frac{2N}{R} = 1.2x10^5\, Pa \cong 1200 cm H_2O$$

a remarkably high value of pressure given the thickness of the membrane is only 6 nm!

Cells also often exhibit an intrinsic surface tension. Reported values are small, however, lying in the range of about 10^{-5} to 10^{-4} N/m (Sheets, Simson et al. 1995). For comparison, recall that the surface tension across the interface of a droplet of pure water is about 0.07 N/m, a value close to the rupture stress of the membrane given above. It becomes immediately obvious, then, that the tension of a cell membrane must be orders of magnitude smaller than the surface tension

[1] This discussion neglects the effects of thermal fluctuations in the membrane that give rise to a much more compliant behavior at the smallest areal strains. When surface stress is sufficient to smooth out most thermal fluctuations, the cell or vesicle will exhibit the large moduli given here. See also Example xx later in this chapter.

of a typical gas-liquid or liquid-liquid interface since it would otherwise give rise to intracellular pressures on the order of one atmosphere!

Pure bending. By contrast, lipid bilayers exhibit a very low bending stiffness; so low that it is often neglected in models of membrane mechanics. It can be important in certain situations, however, and is essential for example in analyzing the thermal fluctuations of vesicles, discussed later in this chapter.

Bending stiffness arises from the same type of molecular interactions that cause extensional stiffness. When an initially flat bilayer is bent, the hydrophilic head groups on the outside of the bend move further apart while on the inside, intermolecular spacing decreases; both represent departures from the equilibrium, unstressed state and require energy. If the same forces of interaction are responsible, why then is bending stiffness so low? While the answer to this question is not simple, one factor is the membrane thickness, which you recall, is only about 6 nm. As the membrane bends, therefore, the change in the surface area per molecule is extremely small, so the associated extensional strains are also minute.

Returning to our simple continuum plate model, consider a bending moment applied to the two ends, causing the plate to curve slightly (Fig. 3.1.6). If the bending is due to moments applied at the two ends about the x_2-axis, then the bending moment per unit length is related to the deflection by

$$M_\alpha = -\frac{Et^3}{12(1-\nu^2)}\left(\frac{\partial^2 u_3}{\partial x_\alpha^{\,2}}\right) = -K_B\left(\frac{\partial^2 u_3}{\partial x_\alpha^{\,2}}\right) \tag{2.5}$$

where K_B is termed the *bending stiffness* having units of N·m . Implicit in this expression are the assumptions that there exists a mid-plane (the "neutral plane") on which the in-plane stress and strain are both zero, and that straight lines perpendicular to this mid-plane remain straight and normal to this surface after deformation.

Typical values for the bending stiffness K_B lie in the range of 10^{-19} N·m (10^{-12} dyn·cm) for a red blood cell or lipid bilayers (Mohandas & Evans, 1990). This value is larger, on the order of 1-2x10^{-18} N·m (Zhelev, Needham et al. 1994), for other cell types (e.g., neutrophils, endothelial cells) that possess a more extensive cortex. The methods used to obtain these values will be described later in this chapter.

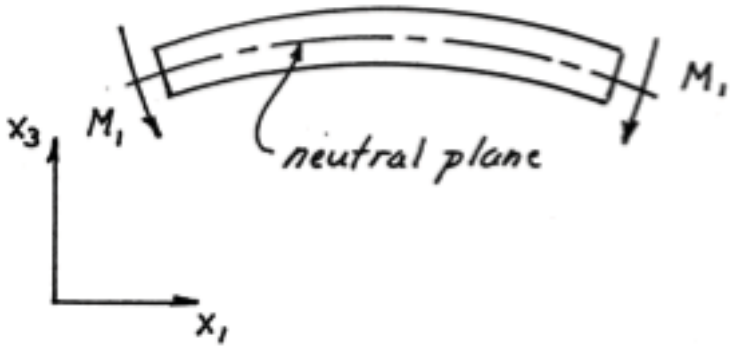

Fig. 3.1.6. Plate subjected to equal moments M_1 at the two edges.

Example. Estimate the moment per unit length acting within an initially flat lipid bilayer (at zero temperature) associated with a wavelength $\lambda = 5$ μm and amplitude $\varepsilon = 1$ μm.

Membrane displacement can be approximated by the expression:

$$u_3 = \varepsilon \sin(2\pi x_1 / \lambda) \tag{2.6}$$

From eqn. (2.5) above, we obtain

$$M_1 = K_B \varepsilon \left(\frac{2\pi}{\lambda}\right)^2 \sin(2\pi u_3 / \lambda) \tag{2.7}$$

Using the values given above, the maximum moment per unit length is 0.158 pN.

Pure shear. Shear deformations arise when a membrane is stretched in one direction by a surface tension N_1 (units of force/length) while the lateral surface contracts under a lesser tension N_2, at constant surface area and in the absence of bending (Fig. 3.1.7). Surfaces oriented at 45 degrees to the boundaries experience pure shear stresses of magnitude $(N_1 - N_2)/2$.

When subjected to shear stresses in the plane of the membrane, a pure lipid bilayer behaves essentially as a liquid. It exhibits a membrane viscosity in that it poses a resisting force proportional to the *rate* of shear deformation, but only a small shear modulus to *static* shear deformations. It is not clear, in fact, whether or not pure lipid bilayers exhibit a non-zero shear modulus. For example, the movement of membrane-bound proteins can be described by a simple diffusion coefficient proportional to the membrane viscosity. Typical cell membranes *do* exhibit a shear modulus, however, largely due to the cortex of cytoskeletal filaments that lie on the intracellular side of the membrane. In a red blood cell this matrix, as discussed above,

consists of interconnected filamentous spectrin and actin with attachments to the membrane via ankyrin.

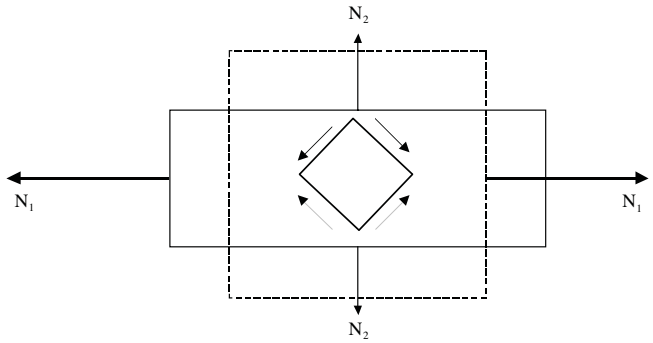

Fig. 3.1.7. A section of membrane subjected to a shear stress of magnitude N_1-$N_2/2$.

The equations relating shear stress to shear deformation (Hooke's law) from Ch. xx can be applied here

$$\tau_{12} = \tau_{21} = 2G\varepsilon_{12} \tag{2.8}$$

or, expressed as a shear force per unit length of membrane:

$$N_{12} = \tau_{12}h = 2G\varepsilon_{12} = K_s\varepsilon_{12} \tag{2.9}$$

where we define the membrane shear modulus, K_s, with units of N/m. Typical values lie in the range of 6-9 x 10^{-6} N/m for a red blood cell membrane. A pure lipid bilayer exhibits a *viscous* resistance to shear deformations characterized by a shear viscosity of about 10^{-6} N·s/m ((Evans 1983)).

The 2D elastic plate -- equations of deformation

In the analysis of cellular membranes, several unique characteristics need to be taken into account.

1. The membrane is extremely thin relative to its lateral extent. If we consider the thickness to be that of the lipid bilayer by itself, then h can be as small as 6 nm compared to a typical cell dimension on the order of 10's of μm. Even if we include the sub-membrane cortex, this

dimension only increases to about 100 nm. This tends to favor in-plane stresses over bending effects[2].

2. The non-shear deformations are very small with strains of at most a few percent. Therefore, linear analysis is appropriate in many situations. Note, however, that nonlinear effects can be important, especially for large shear deformations such as occur in micropipet aspiration of red blood cells. The implications and limitations of this are discussed more fully below.
3. The membrane exhibits a very small modulus in plane shear and is often treated as a two-dimensional liquid. While this applies primarily to lipid bilayers, when the membrane is considered to include the cortex, greater values of shear modulus can be observed.
4. Stresses normal to the membrane are small and can be neglected.
5. Membrane motions can be damped either due to viscous dissipation within the bilayer as in the case of in-plane shear, or due to the viscosity of the fluids on the intra- or extracellular sides of the membrane. These latter are especially important when considering motions of the membrane perpendicular to its plane.
6. Inertial effects can be neglected due to the predominance of viscous forces during transient deformations.

With these in mind, and acknowledging the limitations of a continuum view of such structures, we treat the membrane as a thin, homogeneous plate or membrane in which all the following must be considered: in-plane extension and shear, bending, viscous damping, and thermal fluctuations.

The equations we derive will effectively be integrated through the membrane thickness so that stresses will be in terms of surface forces (force / unit length). These are the in-plane normal forces (see Fig. 3.1.8 for definition of the axes and nomenclature) are therefore written as

$$N_\alpha = \int_{-h/2}^{+h/2} \sigma_\alpha dx_3 \tag{2.10}$$

where h is the membrane thickness, and the vertical shearing forces:

$$V_\alpha = \int_{-h/2}^{+h/2} \tau_{\alpha 3} dx_3 \tag{2.11}$$

The moments acting on the plate edges can be calculated from

[2] Whether tension or bending dominates clearly depends on the nature of the experiment. If an initially spherical cell is distended, tension is most important; if the cell shrinks so that the membrane buckles, bending effects will be critical.

$$M_{\alpha\beta} = \int_{-h/2}^{+h/2} x_3 \tau_{\alpha\beta} dx_3 \tag{2.12}$$

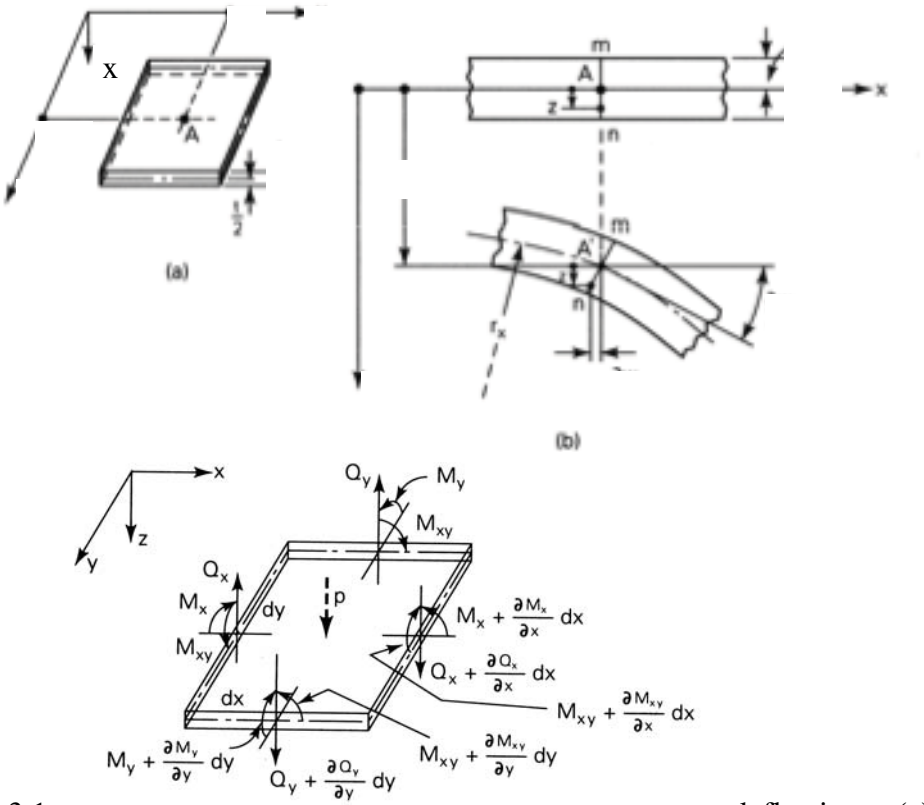

Fig. 3.1.8. (a) A small section of membrane. (b) Membrane deflections. (c) Nomenclature used in defining the forces acting on a section of membrane. (Note that Q is used to represent shear stress in the figure whereas V is used in the text, and (x,y,z) should be (x_1,x_2,x_3).)

In order to distinguish the effects of bending from those giving rise to extension, we separate the normal stress into two parts, one representing the mean over the thickness of the membrane, which is simply N_i/h, and the other representing the deviation from this value, denoted as σ'_α. Similarly, we separate the displacement on the neutral plane, $u_{n\alpha}$ from that which varies with x_3, denoted as u'_α. Consequently, we can write:

$$u_\alpha = u_{n\alpha} + u'_\alpha \quad \text{and} \qquad \sigma_\alpha = \frac{N_i}{h} + \sigma'_\alpha \tag{2.13}$$

And, consistent with the assumption that planar edges initially normal to the membrane remain planar under bending deformations, we have that

$$u'_\alpha = -x_3 \frac{\partial u_3}{\partial x_\alpha} \tag{2.14}$$

According to assumption (4) above, the relationships between stress and strain become:

$$\sigma_\alpha = \frac{E}{1-\nu^2}\left(\varepsilon_\alpha + \nu\varepsilon_\beta\right) \qquad \alpha \neq \beta \tag{2.15}$$

and

$$\tau_{\alpha\beta} = \frac{E}{(1+\nu)}\varepsilon_{\alpha\beta} \qquad \alpha \neq \beta \tag{2.16}$$

Since

$$\varepsilon_\alpha = \frac{\partial u_\alpha}{\partial x_\alpha} = \frac{\partial u_{n\alpha}}{\partial x_\alpha} + \frac{\partial u'_\alpha}{\partial x_\alpha} \tag{2.17}$$

(summation convention not used). We eventually obtain the following expressions for the bending moment:

$$M_\alpha = \int_{-h/2}^{+h/2} \sigma_\alpha x_3 dx_3 = -K_B\left(\frac{\partial^2 u_3}{\partial x_\alpha^2} + \nu\frac{\partial^2 u_3}{\partial x_\beta^2}\right) \qquad \alpha \neq \beta \tag{2.18}$$

and

$$M_{12} = \int_{-h/2}^{+h/2} \varepsilon_{12} x_3 dx_3 = -K_B(1-\nu)\frac{\partial^2 u_3}{\partial x_1 \partial x_2} \tag{2.19}$$

where, in classical shell theory for continuum materials, $K_B = Eh^3/(1-\nu^2)$. The moments are related to the shear forces in the plane of the membrane through a moment balance about the x_1 axis, giving:

$$\frac{\partial M_{12}}{\partial x_1} + \frac{\partial M_2}{\partial x_2} - V_2 = 0 \tag{2.20}$$

so that

$$V_2 = -K_B\frac{\partial}{\partial x_2}\left(\frac{\partial^2 u_3}{\partial x_1^2} + \frac{\partial^2 u_3}{\partial x_2^2}\right) \text{ and } V_1 = -K_B\frac{\partial}{\partial x_1}\left(\frac{\partial^2 u_3}{\partial x_1^2} + \frac{\partial^2 u_3}{\partial x_2^2}\right) \tag{2.21}$$

A force balance in the direction normal to the membrane yields:

$$\frac{\partial V_1}{\partial x_1}+\frac{\partial V_2}{\partial x_2}+\frac{\partial}{\partial x_1}\left(N_1\frac{\partial u_3}{\partial x_1}\right)+\frac{\partial}{\partial x_2}\left(N_2\frac{\partial u_3}{\partial x_2}\right)+p=0 \tag{2.22}$$

which, upon substitution for V_1 and V_2 from eqns. (2.21) becomes:

$$K_B\left(\frac{\partial^4 u_3}{\partial x_1^4}+2\frac{\partial^4 u_3}{\partial x_1^2\partial x_2^2}+\frac{\partial^4 u_3}{\partial x_2^4}\right)-\frac{\partial}{\partial x_1}\left(N_1\frac{\partial u_3}{\partial x_1}\right)-\frac{\partial}{\partial x_2}\left(N_2\frac{\partial u_3}{\partial x_2}\right)-p=0 \tag{2.23}$$

Recall that the first term in parentheses is due to bending, the second and third terms are due to in-plane extension, and the fourth term represents the pressure difference across the membrane.

Eqn. (2.23) contains three unknowns: the displacement u_3 and the two normal forces per unit length, N_1 and N_2. Fortunately, the additional equations required for solution are quite easy to obtain from simple force balances in the x_1 and x_2 directions. Setting the sum of forces in the x_1 direction equal to zero, we obtain (referring to Fig. 3.1.9):

$$-N_1(x_1)+N_1(x_1+dx_1)\cos\theta(x_1+dx_1)-N_{21}(x_2)+N_{21}(x_2+dx_2)=0 \tag{2.24}$$

or

$$\frac{\partial N_1}{\partial x_1}+\frac{\partial N_{21}}{\partial x_2}=0 \quad \text{and similarly} \quad \frac{\partial N_2}{\partial x_2}+\frac{\partial N_{12}}{\partial x_1}=0 \tag{2.25}$$

While formidable in its complete form, it is reassuring to know that we rarely use eqn. (2.23) in its entirety, and that when certain limiting cases are considered, more familiar equations are obtained. It is useful, at this stage, to consider several of these limits.

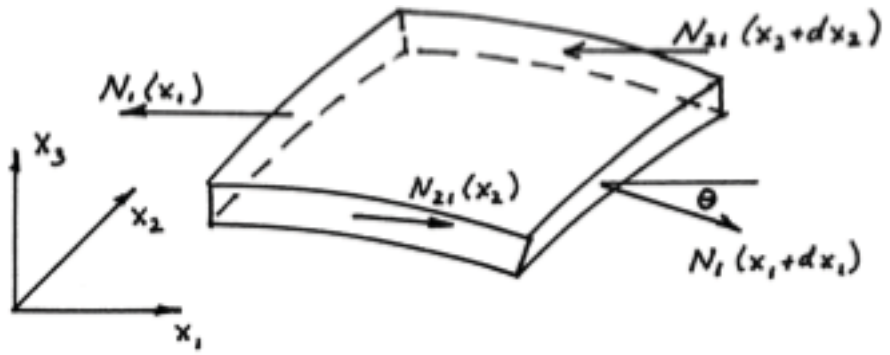

Fig. 3.1.9. x_1 force balance in the plane of the membrane.

Balance between pressure and surface tension (Laplace's Equation). If the in-plane stress is uniform (N_i=N_j=N), eqn. (2.23) has the form:

$$K_B\left(\frac{\partial^4 u_3}{\partial x_1^4}+2\frac{\partial^4 u_3}{\partial x_1^2\partial x_2^2}+\frac{\partial^4 u_3}{\partial x_2^4}\right)-N\left(\frac{\partial^2 u_3}{\partial x_1^2}+\frac{\partial^2 u_3}{\partial x_2^2}\right)-p=0\ , \tag{2.26}$$

and eqn. (2.25) is trivially satisfied. If, in addition, bending stiffness can be neglected, then

$$p=-N\left(\frac{\partial^2 u_3}{\partial x_1^2}+\frac{\partial^2 u_3}{\partial x_2^2}\right)\cong N\left(\frac{1}{R_2}+\frac{1}{R_1}\right), \tag{2.27}$$

for small curvatures, where R_1 and R_2 are the radii of curvature of the membrane about the x_1 and x_2 axes, respectively. This is the well-known Laplace's equation with N the surface tension. For a sphere, $R_1 = R_2$ and the equation simplifies further, yielding the equation given on p. 10.

Balance between pressure and bending. Alternatively, if all in-plane stresses can be neglected, other than those associated with bending stiffness, we obtain the equation generally used for simple bending of plates and shells:

$$K_B\left(\frac{\partial^4 u_3}{\partial x_1^4}+2\frac{\partial^4 u_3}{\partial x_1^2\partial x_2^2}+\frac{\partial^4 u_3}{\partial x_2^4}\right)=p \tag{2.28}$$

Both of these forms will be used later in this chapter to examine specific problems in cell membrane mechanics.

The conditions under which eqn. (2.26) can be reduced to either (2.27) or (2.28) can be determined by an order of magnitude comparison of the bending and tension terms. If we take $\overline{u}$ to be a measure of the membrane displacement in the x_3 direction and λ to be the characteristic length in the x_1 or x_2 directions over which u_3 varies, then the bending term can be shown to scale as $K_B\overline{u}/\lambda^4$ and the tension term as $N\overline{u}/\lambda^2$. The ratio of these tells us which of the terms dominate in eqn. (2.26). If

$$\frac{K_B\overline{u}/\lambda^4}{N\overline{u}/\lambda^2}=\frac{K_B}{N\lambda^2}<<1$$

then tension dominates and eqn. (2.27) is appropriate. Alternatively, if

$$\frac{K_B}{N\lambda^2}>>1$$

then bending dominates, and eqn. (2.28) should be used. If we take values typical of those given for cells: $K_B = 10^{-18}$ N·m, $N = 5\text{x}10^{-5}$ N/m, $\lambda = 1$ μm; this ratio equals 0.02, confirming, as we originally postulated, that tension tends of dominate.

Nonlinear formulations

Traditionally, membrane deformations have been addressed through nonlinear analysis, allowing for large strains, especially in shear. Here we have chosen to present the linearized equations in the hope that they will provide clearer insight, and for continuity with the approach used in other chapters of the text. For many problems of interest, deformations are small and linear theory is sufficiently accurate. In some circumstances, however, a nonlinear analysis is necessary, one example being the aspiration of a red blood cell membrane into a micropipet. For this reason, we present the nonlinear equations in Appendix A for the more advanced reader and to assist in reading the recent literature on membrane mechanics.

Energies of deformation

Although the formulation of the equations of deformation in Section 3.1.6 is complete by itself, an alternative approach is often useful in which we consider the *strain energy*, the energy stored in the membrane due to elastic deformation, as a basis for analysis. Strain energy is analogous to the energy stored in a spring by stretching it. If the spring is linear with a stiffness k, so that the force F required to lengthen it from x_0 to x is $k(x\text{-}x_0)$, then the energy expended during the process of lengthening is

$$U = \int_{x=x_0}^{x} F dx = \int_{x=x_0}^{x} k(x - x_0) dx = \tfrac{1}{2} k(x - x_0)^2 \tag{2.29}$$

Extensional energy. Now consider a section of an elastic membrane of thickness h and lengths dx_1 and dx_2 subjected to a uniaxial tension stress σ_1. Here, as in our previous discussion, we consider two cases, first a flat membrane which is being stretched by extensional stresses (the case at zero temperature), and second, the situation in which the surface area of the membrane projected onto a flat plane, increases due to the smoothing of out-of-plane undulations (the entropic contribution).

As the stress is gradually applied, to minimize any dissipative effects, the work done by the external force must equal the gain in elastic energy stored in the plate. The work performed by this stress is

$$dU = \int_0^{\varepsilon_1} \sigma_1 d\varepsilon_1 dx_1 dx_2 dx_3 = \int_0^{\varepsilon_1} E\varepsilon_1 d\varepsilon_1 dx_1 dx_2 dx_3 \tag{2.30}$$

By energy conservation, the work done in stretching the membrane must be stored, as potential or strain energy in the elastic member. Since the right-hand-side of (3.30) represents the strain energy in the volume $dx_1 dx_2 dx_3$, then the energy per unit volume of membrane is

$$U_0 = \int_0^{\varepsilon_1} \sigma_1 d\varepsilon_1 = \int_0^{\varepsilon_1} E\varepsilon_1 d\varepsilon_1 = \tfrac{1}{2} E\varepsilon_1^2 \tag{2.31}$$

or, expressed as energy per unit area of membrane:

$$U_0 h = \frac{Eh\varepsilon_1^2}{2} \tag{2.32}$$

In the somewhat more general case of biaxial strain, a similar approach leads to

$$U_0 h = \frac{Eh}{2(1-\nu)}\left(\varepsilon_1^2 + \varepsilon_2^2\right) = \frac{Eh}{2(1-\nu)}\left[\left(\frac{\partial u_1}{\partial x_1}\right)^2 + \left(\frac{\partial u_2}{\partial x_2}\right)^2\right] \tag{2.33}$$

Note that if the strain is isotropic in that $\varepsilon_1 = \varepsilon_2 = \varepsilon$, this can also be expressed in terms of the areal strain with the aid of eqn. (2.3)

$$U_0 h = \frac{Eh}{4(1-\nu)}\left(\frac{\Delta A}{A_0}\right)^2 \quad , \tag{2.34}$$

from which it can be seen by eqn. (2.4) that the area expansion modulus has the form:

$$K_e = \frac{Eh}{2(1-\nu)} \tag{2.35}$$

under the assumptions of a homogeneous, isotropic elastic membrane. This term, however, only accounts for the contribution to extensional energy associated with an increase in the surface area of a membrane. Another contribution arises from the change in the membrane surface area *projected onto the x_1-x_2 plane*, due to non-uniform displacements perpendicular to the plane of the membrane, in the x_3 direction. This can be seen from the following one-dimensional example.

Consider a membrane, tethered at both ends that exhibits a *constant* surface tension N when deformed into a new state defined by $u_3(x_1)$. Locally, the change in length of a segment, initially of length dx is:

$$\sqrt{(dx)^2+(du_3)^2}-dx=\left[1+\left(du_3/dx_1\right)^2\right]^{1/2}dx_1-dx_1\approx\left(1+\tfrac{1}{2}\left(du_3/dx_1\right)^2\right)dx_1-dx_1=\tfrac{1}{2}\left(du_3/dx_1\right)^2dx_1 \tag{2.36}$$

[see also Figs. 6.4 and 6.5 in Boal] The strain is then the change in length over the initial length, or:

$$\varepsilon_{11}=\tfrac{1}{2}\left(du_3/dx_1\right)^2 \tag{2.37}$$

and the energy per unit area associated with this change in length under a constant tension N is

$$U_0h=N_1\int_0^{\varepsilon}d\varepsilon=\frac{N}{2}\left(\frac{\partial u_3}{\partial x_1}\right)^2 \tag{2.38}$$

which, extending to two dimensions, can be written:

$$U_0h=\frac{N}{2}\left[\left(\frac{\partial u_3}{\partial x_1}\right)^2+\left(\frac{\partial u_3}{\partial x_2}\right)^2\right] \tag{2.39}$$

It is important to recognize that we now have two expressions associated with the energy of extension, and they represent two distinct phenomena. The first [eqn. (3.33)] describes the energy associated with true areal expansion; that is, a change in the effective spacing between the molecules comprising the lipid bilayer. The second [eqn. (3.39)] corresponds to the energy change due to undulations in a membrane with *constant* intermolecular spacing. To see the distinction between the two, consider an experiment in which the pressure inside a cell or a lipid vesicle is gradually increased by aspiration into a micropipette. Initially, the *projected* area of the membrane rises rapidly with a relatively small increase in membrane tension, corresponding to the smoothing of undulations caused by thermal excitation of the membrane. This is followed at higher tensions by a transition to a regime in which the membrane exhibits a much greater stiffness, corresponding to the situation in which the thermally-induced undulations have been smoothed out, and the true membrane surface area now must increase. In the absence of thermal fluctuations, e.g., at zero temperature, only this second regime would be observed. [see also figure from Boal]

Energy of shear deformation. Next examine the energy per unit area associated with shear deformation in the plane of the membrane, which can be expressed in the form:

$$U_0h=\tfrac{1}{2}h\tau_{12}\varepsilon_{12}=\tfrac{1}{2}hG\varepsilon_{12}^2=\frac{Gh}{2}\left(\frac{\partial u_1}{\partial x_2}+\frac{\partial u_2}{\partial x_1}\right)^2 \tag{2.40}$$

where we have utilized eqns. (2.8) and (2.9) to obtain a form similar to that of eqn. (2.34) for extensional deformation.

[See Boal for an alternative form in terms of membrane curvature. He also gives a nice description of bending in bilayer membranes.]

Bending energy. The contribution due to bending energy is somewhat more difficult to derive. First, recognize that only those normal stresses that vary with x_3 contribute to the bending energy; that is, those contributed by the σ' stresses in eqn. (2.13). With this in mind, we can write the expression for the total elastic energy due to bending as:

$$U = \iiint \left\{ \frac{1}{2E}\left[\left(\sigma_1'\right)^2 + \left(\sigma_2'\right)^2 + 2\nu\sigma_1'\sigma_2' \right] + \frac{1}{2G}\left(\tau_{12}'\right)^2 \right\} dx_1 dx_2 dx_3 \tag{2.41}$$

Substituting for the stresses and strains from eqns. (2.15)-(2.17), this can be re-cast in the following form:

$$U = \frac{K_B}{2} \iint \left\{ \left(\frac{\partial^2 u_3}{\partial x_1^2} + \frac{\partial^2 u_3}{\partial x_2^2} \right)^2 - 2(1-\nu) \left[\frac{\partial^2 u_3}{\partial x_1^2}\frac{\partial^2 u_3}{\partial x_2^2} - \left(\frac{\partial^2 u_3}{\partial x_1 \partial x_2} \right)^2 \right] \right\} dx_1 dx_2 \tag{2.42}$$

It can be shown ((Meleard 1998)) that the integral of the second term in the integrand above [the one multiplied by *2(1-ν)*] is globally constant under deformation if the membrane remains a closed surface with no holes. Assuming that to be the case, we obtain for the total bending strain energy,

$$U = \frac{K_B}{2} \iint \left(\frac{\partial^2 u_3}{\partial x_1^2} + \frac{\partial^2 u_3}{\partial x_2^2} \right)^2 dx_1 dx_2 + const \tag{2.43}$$

Since we typically are concerned with *changes* in energy, the constant will arbitrarily be set to zero. Thus, the energy per unit area, or *energy density of bending deformations*, can be written,

$$U_0 h = \frac{K_B}{2} \left(\frac{\partial^2 u_3}{\partial x_1^2} + \frac{\partial^2 u_3}{\partial x_2^2} \right)^2 \tag{2.44}$$

Note that the term in parentheses is proportional to the mean curvature of the surface. Often, the surface has a natural mean curvature in the unstressed state. If that curvature is c_0, the bending energy expression is modified slightly to the form:

$$U_0 h = \frac{K_B}{2}\left(\frac{\partial^2 u_3}{\partial x_1^2} + \frac{\partial^2 u_3}{\partial x_2^2} - c_0\right)^2 \tag{2.45}$$

Another common form of this expression is obtained by recognizing that the first two terms in parentheses represent the linearized form of the sum of the principal curvatures (the largest and smallest curvatures at a point), denoted c_1 and c_2, so that eqn. (3.45) can be written:

$$U_0 h = \frac{K_B}{2}\left(c_1 + c_2 - c_0\right)^2$$

Although each of these expressions for strain energy density has been derived individually, they of course all contribute in the general situation and are linearly additive. In that regard, several points are worthy of note. First, one can obtain some idea of the relative importance of extension, shear, and bending deformations in a given situation simply by comparing their relative energies, just as was done in the last section by comparison of the bending and tension terms in eqn. (2.26). Not surprisingly, the comparison leads to the same expressions we obtained before for when either bending or tension is dominant. Second, due to the small shear modulus of most cell membranes, the energy stored in shear deformation can generally be neglected. And finally, a comment is warranted concerning the energy due to tension. Various simplifying assumptions can be made, depending on the cell type being considered and the nature of the stress to which the cell (or vesicle) is being subjected, but generally the lipid bilayer can be considered to be of constant area unless it experiences grossly non-physiologic levels of stress. Thus, the main contribution to extensional energy is that represented by eqn. (3.39), associated with the smoothing of membrane undulations.

Other Factors Influencing Membrane Motion

Thermal fluctuations. Biological membranes of all types can be seen to fluctuate due to Brownian motion of the surrounding molecules, if viewed with sufficient resolution. These fluctuations are, in fact, often used to measure the membrane bending stiffness since thermal effects are seen as motions in the membrane of relatively long wavelength, favoring bending energies as compared to extensional or shear (see eqn. (2.23)). To account for these effects, it is customary to add a time-dependent forcing term to eqn. (2.23), $\eta(t)$, the magnitude of which scales with $k_B T$. We analyze thermal motions later, and use them as a means of determining the bending stiffness of a membrane.

Damping due to external fluids. When a membrane fluctuates in a direction perpendicular to its plane, velocities are induced in the surrounding fluids and, due to the resulting shear stresses, energy is dissipated. These motions are extremely complex to model precisely, and depend on both the nature of the surrounding medium (its rheological properties) and the bounding geometry. In lieu of a complete and rigorous analysis, a local damping term is sometimes added to the membrane force balance equation (eqn. (2.23)) to approximate these effects. Its form is based on the presumption that externally induced velocities scale with the velocity of the wall, and that shear forces in the external fluid scale with the induced shear rates and velocities. Accordingly, eqn. (2.23) is modified by the addition of a term of the form $\mu_m \partial u_3 / \partial t$ where μ_m is the effective viscosity of the external fluid. The equation that results from the addition of both thermal forcing and external fluid viscosity is:

$$\mu_m \frac{\partial u_3}{\partial t} + K_B \left(\frac{\partial^4 u_3}{\partial x_1^4} + 2 \frac{\partial^4 u_3}{\partial x_1^2 \partial x_2^2} + \frac{\partial^4 u_3}{\partial x_2^4} \right) - \frac{\partial}{\partial x_1} \left(N_1 \frac{\partial u_3}{\partial x_1} \right) - \frac{\partial}{\partial x_2} \left(N_2 \frac{\partial u_3}{\partial x_2} \right) = p + \eta(t) \qquad (2.46)$$

An expression of similar form for a linear polymer is sometimes referred to as the *Rouse equation*.

3.1.4 Measurements of Membrane Elastic Parameters

Although the analogy has limitations, it is useful at the onset to think of the cell as a fluid-filled balloon or bag. Just as in the case of a balloon, the elastic properties of the membrane can be determined by any experiment in which the membrane tension changes while its area is measured. In the simple example of a spherical balloon, tension can be computed from the inflating pressure and the measured radius, the latter also yielding the surface area. Ignoring for now the thermal-induced fluctuations in a real cell membrane (ie., assuming the cell to be at zero temperature), the calculations become particularly simple. Furthermore, we will consider cells for which the cytoplasm can be considered to fluid-like having no elasticity. We return to address both issues shortly.

Osmotic swelling

Perhaps the simplest method to inflate the cell and measure the membrane elastic properties is to cause the cell to swell by changing the osmolarity of the external fluid and simultaneously monitoring the change in cell volume. The change in transmembrane pressure mirrors the

change in osmotic pressure brought about by successive additions of a solute to which the membrane is impermeable. For ions and small molecules, the osmotic pressure π can be calculated from the van't Hoff equation

$$\pi = RT\sum_i C_i \tag{2.47}$$

where C_i are the molar concentrations of all solutes to which the membrane is impermeable. For larger molecules such as proteins, their contribution to osmotic pressure is much larger than indicted by this equation.

Consider for example a spherical cell expanded osmotically so that the internal hydrostatic pressure, relative to external pressure, is p_c. Microscopic examination yields a value for the cell radius, R_c. Using these values in combination with Laplace's law [eqn. (2.27)] gives us the tension in this state, and eqn. (2.4) provides its relationship to the extensional modulus:

$$N = \frac{p_c R_c}{2} = K_e \frac{\Delta A}{A_0} \tag{2.48}$$

The observed change in radius allows calculation of ΔA. In practice, identification of the reference state at zero p_c is problematic due to the presence of thermal fluctuations, but if K_e can be assumed constant for relatively small changes in area, it is possible to extrapolate back to the zero-stress state from two measurements at elevated p_c. [Example: red blood cell.]

Micropipet aspiration.

One of the first methods used to measure the extensional modulus of the cell membrane involved drawing a cell, slightly deflated, into a micropipet, simultaneously monitoring the dimensions of the cell and the pressure in the micropipet (Daily, Elson et al. 1984). Since, on the time scale of the experiment, the volume of the cell could be assumed constant, the shape change due to aspiration of the cell causes increases in both internal pressure and surface tension, both of which are assumed spatially uniform. Once the tension is large enough (or the temperature low enough) to dampen the amplitude of any thermal fluctuations, the cell can be treated assuming that membrane extension is the dominant means by which the pressure drop across the membrane is balanced. [For further discussion on the thermal fluctuations and the relationship between micropipet pressure and intracellular pressure, see Daily, and Evans and Rawicz, Phys Rev, 1990. See also figure on p. 199 of Boal. Example: the two regimes in membrane stiffness.]

For the situation shown in Fig.xx, the cell is drawn into the micropipet to the point at which the portion of the cell external to the cell is spherical, of radius R_c. With the assumptions

stated above, the (uniform) pressure within the cell can be related to it surface tension (assumed uniform) and the radii of curvature of the main body of the cell, R_c, and the portion inside the pipet, a, using Laplace's law [eqn. (2.27)]:

$$p_c = 2N / R_c = -\Delta p + 2N / a \tag{2.49}$$

where pressures are referenced to the external, ambient pressure. Reorganizing to solve for surface tension we obtain:

$$N = \frac{\Delta p}{2\left(\frac{1}{a} - \frac{1}{R_c}\right)} \tag{2.50}$$

The surface area corresponding to a given N is obtained from geometry, summing the membrane surface areas of the cylinder and hemisphere inside the micropipet, and the truncated spherical surface outside yielding, for the areal strain the approximate expression:

$$\frac{\Delta A}{A} \cong \frac{\left[(a/R_c)^2 - (a/R_c)^3\right]\Delta L}{2a}$$

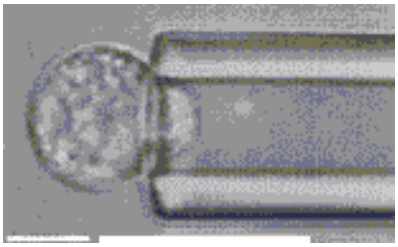

Fig. xx Micropipet aspiration of a neutrophil.

This relationship between N and $\Delta A/A$ can be used to calculate the area expansion modulus,

$$K_e = \frac{Eh}{2(1-\nu)} = N\frac{A_0}{\Delta A}$$

where the expression involving Young's modulus assumes the membrane to be isotropic and homogeneous. The relationship could, however, be non-linear in that the value of K_e may vary with the degree of area expansion; a linear relationship between N and ΔA yields a constant value for K_e.

It is important to note that neither of these approaches, osmotic inflation or micropipet aspiration provides us with any information on the bending modulus. To be precise, bending

does play a role in the micropipet experiments, but the effects are so small as to be negligible and are typically ignored. That is not to say that bending is always negligible, however, as discussed next.

Monitoring thermal fluctuations in the membrane.

When a cell or lipid vesicle is observed floating free, unattached to a substrate, it can be seen to exhibit time-dependent undulations as a result of collisions with the surrounding molecules undergoing thermal motion. In the case of a lipid vesicle with diameter in the range of 10 microns, these undulations can be readily observed microscopically. In smaller cells such as red blood cells, the motions can be inferred from the flickering phenomenon associated with the light interference as the cell thickness changes (Zeman, Engelhard et al. 1990). Since the amplitude of the membrane undulations depends on the stiffness of the membrane to bending, and its surface tension, it is reasonable to expect that measures of this amplitude can be used to infer the membrane elastic parameters. In order to illustrate the method, while avoiding some of the algebraic complexity, consider undulations in a flat membrane with significant bending stiffness and a constant surface tension. The relationship between the motion and the elastic properties can be found by considering the total energy of the membrane, obtained by summing the energies per unit area from eqns. (2.39) and (2.44) and integrating over the membrane surface area A_m:

$$\int_{A_m} U_0 h dA = \int_{A_m} \left\{ \frac{K_B}{2}\left(\frac{\partial^2 u_3}{\partial x_1^2} + \frac{\partial^2 u_3}{\partial x_2^2} \right)^2 + \frac{N}{2}\left[\left(\frac{\partial u_3}{\partial x_1} \right)^2 + \left(\frac{\partial u_3}{\partial x_2} \right)^2 \right] \right\} dA \tag{2.51}$$

In writing the energy in this form, we have omitted the contribution due to shear deformation, consistent with the fluid-like character of a pure lipid bilayer, and have taken the surface tension to be uniform during the deformation. In this example, membrane surface area changes only as a result of fluctuations from the mean [$u_3(x_x,x_2) = 0$] configuration; that is, we now ignore the contribution due to changes in intermolecular spacing and only consider changes in the area projected onto the x_1-x_2 plane.

It is convenient to use the method of Fourier transforms to represent the undulations of a membrane normal to the x_1-x_2 plane, which in two-dimensions leads to [see also class notes on bending of cytoskeletal filaments; alternatively, use Fourier series representation]:

$$u_3(\vec{x}) = u_3(x_1,x_2) = \frac{A}{4\pi^2}\int \exp(i\vec{q}\cdot\vec{x}) b(\vec{q}) d\vec{q} = \frac{A}{4\pi^2}\int \exp(iq_1x_1)\exp(iq_2x_2) b(q_1,q_2) dq_1 dq_2 \tag{2.52}$$

where $q_\alpha = 2\pi/\lambda_\alpha$ is the wavenumber of the particular mode and $b(q)$ is the continuous analogue of the discrete coefficients that multiply each mode in a Fourier series representation. Here the algebra gets complicated, so only the results of the analysis will be presented, however those wishing to see a more complete derivation should see (Boal, *Mechanics of the Cell*, Cambridge University Press, 2002). Introducing eqn. (3.52) into (3.51) yields:

$$\int U_0 h dA = \frac{1}{2}\left(\frac{A}{2\pi}\right)^2 \int \left(K_B q^4 + N q^2\right) b(q) b^*(q) dq \tag{2.53}$$

where $b^*(q)$ is the complex conjugate of $b(q)$. Now we invoke a previous result, that at equilibrium, energy is equally distributed among the various modes, and that each mode has an average energy of $k_BT/2$. Taking the ensemble average of eqn. (3.53) and equating the energy of each mode represented in the result to $k_BT/2$ (by the equipartition theorem) leads to:

$$\left\langle b(q) b^*(q) \right\rangle = \frac{k_B T / A}{K_B q^4 + N q^2} \tag{2.54}$$

This is a useful result in itself, demonstrating that all modes tend to be suppressed as temperature falls or as bending stiffness or surface tension rise. In addition, it shows the tendency for higher modes to be of smaller amplitude. But this equation has further value in that it can be used to obtain a direct expression for the change in apparent area of a membrane as tension increases.

Consider the true surface area of a membrane, A, represented as the sum of its projected area and the additional area associated with thermally-induced undulations:

$$A = \int dx + \frac{1}{2}\int \left[\left(\frac{\partial u_3}{\partial x_1^2}\right)^2 + \left(\frac{\partial u_3}{\partial x_2^2}\right)^2\right] dx \tag{2.55}$$

Isolating the term representing the area reduction due to thermal fluctuations, expressing u_3 in terms of its Fourier transform, and taking the ensemble average of the result, leads to:

$$\left\langle A - \int dx \right\rangle = \frac{1}{2}\left(\frac{A}{2\pi}\right)^2 \int q^2 \left\langle b(q) b^*(q) \right\rangle dq \tag{2.56}$$

Combing eqn. (2.54) from above with this expression yields

$$\frac{\left\langle A - \int d\bar{x} \right\rangle}{A} = \frac{k_B T}{8\pi^2} \int \frac{d\bar{q}}{N + K_B q^2} = \frac{k_B T}{8\pi^2} \int \frac{dq^2}{N + K_B q^2} \tag{2.57}$$

where in writing the last term we have introduced the relations $dq = dq^2 d\theta/2$ and $\int d\theta = 2\pi$. By a simple substitution, $z = q^2 + (N/K_B)$the integral can be evaluated. We do so, however, between specified limits on the assumptions that the range of possible wavenumbers is restricted by the size of the membrane on one hand ($q = (\pi/A^{1/2})$) and the distance between individual lipid molecules on the other ($q = \pi/l_m$). Integrating between these limits results in:

$$\frac{\left\langle A - \int d\bar{x} \right\rangle}{A} = \frac{k_B T}{8\pi K_B} \ln\left(\frac{\frac{\pi^2}{l_m^2} + \frac{N}{K_B}}{\frac{\pi^2}{A} + \frac{N}{K_B}} \right) \tag{2.58}$$

If we use the area reduction at zero tension as a reference, and increase the area from that condition by progressively increasing membrane tension, as in a typical experiment, we finally obtain an expression relating the change in area to the change in tension

$$\frac{\Delta A}{A} \equiv \left. \frac{\left\langle A - \int d\bar{x} \right\rangle}{A} \right|_{N=0} - \left. \frac{\left\langle A - \int d\bar{x} \right\rangle}{A} \right|_{N} = \frac{k_B T}{8\pi K_B} \ln\left(\frac{1 + \frac{NA}{\pi^2 K_B}}{1 + \frac{N l_m^2}{\pi^2 K_B}} \right) \cong \frac{k_B T}{8\pi K_B} \ln\left(1 + \frac{NA}{\pi^2 K_B} \right) \tag{2.59}$$

where we have used the assumption, supported by typical values found from different experiments, that $\left(N l_m^2\right)/\left(\pi^2 K_B\right) << 1$.

You should recall, that this solution was obtained on the assumption that the actual area of the membrane remained constant, and that the reduction in projected or apparent area resulted from the undulations being progressively smoothed out. Once the undulations are eliminated, the only means by which the projected area of the membrane can further increase is by an increase in the inter-molecular spacing – an increase in the actual membrane area. When this occurs, we expect to see a transition to the behavior discussed at the beginning of this chapter, a result expressed as:

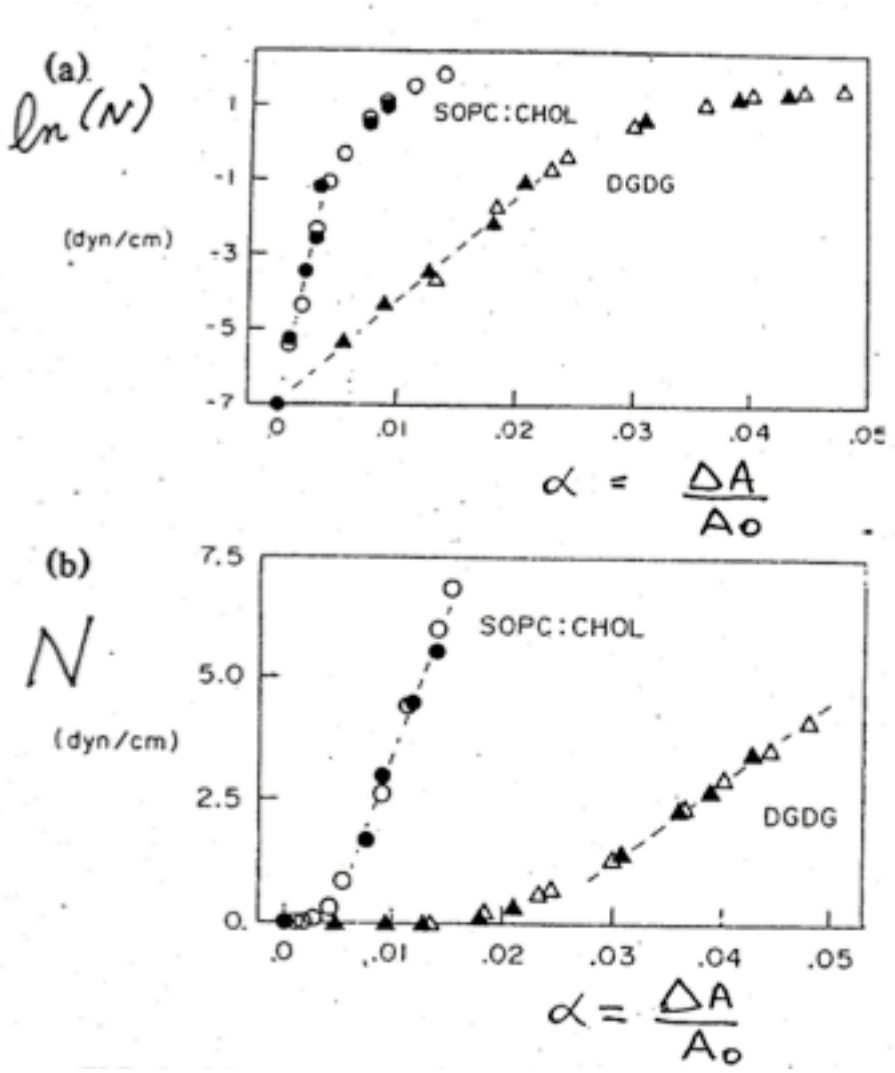

Fig. yy. Plots of tension vs. normalized surface area for lipid vesicles of different composition. Evans & Rawicz, 1990

$$\frac{\Delta A}{A} = \frac{N}{K_e} \tag{2.60}$$

Thus we have two limiting predictions, one for low tensions, eqn. (2.59), and another for high tensions, eqn. (2.60), and the transition from one behavior to the other should occur when the two expressions for $\Delta A/A$ are of the same magnitude. This is supported by experiment (Fig. yy) and the results in the two regimes provide a means for estimating the two moduli, K_e and K_B.

Before leaving this analysis, there is one further result that is useful to state, although the derivation is, again, somewhat involved. Once we have the solution for the undulations at a given level of tension and for given membrane properties, the ensemble average displacement normal to the plane of the membrane can also be computed, with the result:

$$\left\langle u_3^2 \right\rangle = \frac{k_B T}{4\pi N} \ln\left(1 + \frac{NA}{\pi^2 K_B}\right) \tag{2.61}$$

Again, this supports our intuition that the undulations will be suppressed at low temperature or high tension. And in the limit as $N \to 0$, a binomial expansion of the natural log term shows that the effect of tension drops out, and the magnitude of the undulations varies inversely with the bending stiffness.

3.1.5 Membrane Fluid Mechanics

Early studies of protein diffusion, notably the work of Saffman (Saffman 1976), examined protein diffusion using an approach akin to that of Einstein in three dimensional space, thereby reducing the problem to one of solving for the mobility b in the equation for diffusivity:

$$D = k_B T b \tag{2.62}$$

Calculation of the mobility is influenced by the viscous drag on the portion of the protein within the membrane, but also on to the intra- and extracellular domains as well. The solution of interest here is the one applicable in the limit of small μ_e/μ_m where μ_e and μ_m are the external and membrane viscosities, respectively, leading to:

$$D = \frac{k_B T}{4\pi\mu_m h}\left(-\gamma + \ln\frac{h\mu_m}{a\mu_e}\right) \tag{2.63}$$

where h is the membrane thickness, a the radius of the protein (assumed cylindrical) and γ is Euler's constant (=0.5772). Membrane viscosity has been estimated from lipid diffusion to be ~2 poise (McCloskey and Poo 1984). When finite mobility is achieved as a result of a finite domain as, for example, a circle of radius R, the corresponding result is:

$$D = \frac{k_B T}{4\pi\mu h}\left(\log\frac{R}{a} - \frac{1}{2}\right) \tag{2.64}$$

While this represents a useful point of departure, measurements of lateral diffusion in a membrane have demonstrated a more complex behavior. Fluorescence recovery after photobleaching (FRAP) has enabled the direct tracking of membrane proteins labeled with fluorescent antibodies. More recently, single particle tracking methods have been developed using colloidal gold or a fluorescent particle in conjunction with digital microscopy, as well as controlled movements using microbeads manipulated by an optical trap.

From experiments such as these, a new picture has emerged. While the lateral diffusion of lipids and a small fraction of trans-membrane proteins satisfy the general form of Saffman's predictions, the predicted diffusivity is greater than that observed experimentally and agrees with experiments only when a membrane viscosity of 100 poise is used. This might be due to the presence of other proteins in the membrane (Kucik, Elson et al. 1999). Experiments also show that many proteins appear to diffuse freely only in small domains typically measuring from 200-600 nm, remaining confined to these domains for periods on the order of tens of seconds. To explain this behavior, the *membrane skeleton fence* model was proposed (Kusumi, Sako et al. 1993) in which a membrane-associated matrix constrains the movement of proteins outside of the domains defined by the matrix filaments. Diffusion beyond these barrier filaments can occur either as a result of random thermal motions of the transmembrane protein, matrix filaments, or both, or by transient breaks in the filaments. Confinement of proteins may play an important role in rapid and selective signaling. Rapid, directed motion of membrane-associated proteins has also been observed, and is likely due to active transport by an intracellular, actin- or microtubule-based motor.

3.1.6 Cell Adhesion

This section deals with how cells adhere to their surroundings, and through these sites of adhesion, how they interact with the external world. We begin by summarizing the different types of adhesion, their functions and the molecules involved. Next, we provide a brief description of the adhesion complexes found in cells and the role of each type. Then, the theories that provide a quantitative description of adhesion between single receptor-ligand pairs are reviewed in the context of the material presented in Chapter xx including the role of thermal fluctuations. Through these theoretical models, both the static and dynamic states of adhesion can be explored for single molecule pairs, then for adherent cells. Next we develop the different

approaches that are used to study the adhesion of cells, based either on thermodynamics or mechanics. Methods for the measurement of adhesion strength are described, providing estimates for the force that a cell can exert on its surroundings. Various examples will be presented, but the adherence of leukocytes to the endothelium, and the role of adhesion in cell migration will receive special attention.

Functions of adhesion

Adhesion has been found to be an essential process, necessary for a variety of fundamental cellular functions.

- *Structural integrity*. Adhesion helps to maintain the overall structural integrity of the tissue; in muscle, for example, it provides the means of force transmission from the cells to the surrounding matrix to allow contraction. In non-contractile cells, it still provides the needed mechanical coupling to the surrounding tissue, necessary for a variety of cellular functions.
- *External sensing*. Adhesion provides a means by which the cell can sense, and subsequently respond to, its surroundings. Forces transmitted directly to the cell membrane or to the cytoskeleton via transmembrane proteins may trigger a variety of biochemical reactions within the cell as we shall see later, in Chapter 3.3.
- *Migration*. Cell-matrix adhesion is an essential element in cell migration; a cell propels its way through tissue or along a surface through a process involving adhesion, contraction, and release, also described in Chapter 3.3.
- *Regulation of transport*. Sites of cell-cell adhesion are often important in the regulation of transport across a cell layer such as in the case of an epithelium or endothelium.
- *Communication*. Sites of mechanical coupling often provide a means of cell-cell communication, as in the case of gap junctions, which offer a pathway for the diffusion of ions and small molecules between adjacent cells.

Adhesion molecules

Cells adhere to their surroundings or to an artificial substrate via a wide variety of different proteins that can be classified into five major families: integrins, selectins, cadherins, immunoglobulins, and transmembrane proteoglycans (Table 1). In terms of their mechanism of attachment to other cells or the external matrix, these can be classified as either homophillic – binding to like molecules, heterophillic – binding to unlike molecules, or those that bind to other cells through an extracellular linker molecule.

Integrins, one of the largest class of adhesion molecules, are primarily used to attach cells to the extracellular matrix or the basal lamina, but are also present in some cell-cell adhesion

complexes. They typically bind to the matrix via the RGD amino acid sequence (arginine, glycine, aspartic acid) but can also contain other binding motifs. Integrins are heterodimers in that they always contain an α and a β subunit, with the different isoforms determining the specific ligand to which the integrin binds. Two specific types of adhesion, focal adhesions and hemidesmosomes often contain integrins, and the attachments they make can at times be stable, but at other times transient, so as, for example, to mediate cell migration. The force of adhesion of a single integrin-ligand bond has been measured using atomic force microscopy, and found to be in the range of 30-100 pN (Lehenkari and Horton 1999) with a relatively low binding affinity in the range of $K_D \sim 10^{-6}$ to 10^{-8} mol/liter. By comparison, typical cell-surface receptors bind with an affinity in the range of 10^{-9} to 10^{-11} mol/liter. Integrins also play an important role in signaling since extracellular integrin binding is known to influence cytoskeletal morphology as well as the state of cell differentiation.

Adhesion molecules in the selectin family also tend to form transient bonds, and are important in leukocyte adhesion and *extravasation*, the migration of the leukocyte through the endothelium and into the tissue. Consequently, they tend to be found in cells of the circulation, and are present both in leukocytes and endothelial cells and are instrumental in adhesion between these two cell-types during leukocyte rolling.

Family	**Location and/or function**	**Ligands recognized**	**Comments**
integrins	focal adhesions, hemi-desmosomes, leukocyte ("spreading") adhesion, primarily cell-matrix adhesion but also in some cell-cell adhesions	(E) fibronectin, collagen, laminin, immunoglobulins, (I) actin filaments	relatively low affinities ($K_D \sim 10^{-6}$-10^{-8} mol/liter)
selectins	circulating cells and endothelial cells, "rolling" adhesion	carbohydrates	require Ca^{2+}
Ig superfamily (immunoglobulin)	important in immune response	integrins, homophillic	
cadherens	adherens junctions, desmosomes	(E) homophillic, (I) actin	require Ca^{2+}

		filaments, intermediate filaments	
transmembrane proteoglycans	fibroblasts, epithelial cells	(E) collagen, fibronectin (I) actin filaments, heterophillic	bind various growth factors such as FGF

Table 1. Cell adhesion molecules and their characteristics.

While both integrin and selectin binding is mediated by Ca^{2+}, adhesion via the immunoglobulin (Ig) superfamily of proteins is Ca2+ independent. Some of the most prominent members of this family are the N-CAMs (Neural cell adhesion molecules) and ICAMs (Intracellular cell adhesion molecules). These tend to undergo homophillic bonding, but some also bind to members of the integrin family.

Cadherens are often expressed in the same cells as the selectins, but form much stronger bonds and therefore play an important role in maintaining cell integrity. Because of these attributes, cadherens are the primary adhesion proteins in desmosomes and adherens junctions, the major structural contacts cells form with other cells or the basil lamina. These also form homophillic bonds by a Ca^{2+} dependent mechanism and mediate selective bonding between adjacent cells. Cadherens are relatively short as compared to other adhesion molecules, being about 700-750 amino acid residues in length.

Types of adhesion complexes

Cells have developed a variety of specialized adhesion complexes, each utilizing one or more of the adhesion molecules of Table 1 and each serving a specific purpose. Typically, the cell-cell or cell-surface spacing is in the range of 10-20 nm, but this is highly variable ranging from less than 1 nm when controlling transport to over 100 nm in regions where tight control is unnecessary. Below we describe the different types of junctions and, where important for function, their mechanical characteristics.

Gap junctions. Cells need to communicate with their neighbors for a variety of reasons. For example, cardiac myocytes transmit signals from cell to cell in order to maintain a synchronous

wave of contraction. This is typically accomplished by providing a pathway for ions and small signaling molecules between cells called gap junctions (Fig. 3.1.10). These minute channels are typically comprised of a collection of six connexin proteins that cluster together in cylindrical fashion, forming a minute channel that passes molecules and ions less than about 1200 to 2000 MW (1.5-2 nm). Transport through these channels is regulated and their permeability drops in the presence of high Ca^{2+} concentration, as when a cell membrane is ruptured, or with low pH. Cyclic AMP, acting as a second messenger, can be exchanged between cells, therefore gap junctions provide a metabolic linkage between neighboring cells and provide a means by which hormonal stimulation of just one cell can be transmitted to others.

Adherens junctions. Adherens junctions are belt-like structures that can be though of as the structural "weld" that holds two cells together (Fig. 3.1.10). Because of their structural role, these junctions formed by homophilic bonding between proteins in the cadheren family are anchored securely, again via the adaptor proteins, α, β, γ-catenin, to the cytoskeleton.

Desmosomes and Hemidesmosomes. If the adherens junctions are the continuous welds between cells, desmosomes are the "spot welds". Again, these serve primarily a structural purpose, joining two neighboring cells via a complex consisting of a dense plaque on the intracellular sides of both cells extending 15-20 nm into the cell and consisting of a variety of proteins that attach to keratin filaments, part of the intermediate filament network. Hemidesmosomes have similar intracellular structure, but attach instead to the basal laminae. Based on their different extracellular attachment sites, desmosomes typically link to other cells via cadherens whereas hemidesmosomes adhere via a type of integrin. Both are commonly found in epithelial cells.

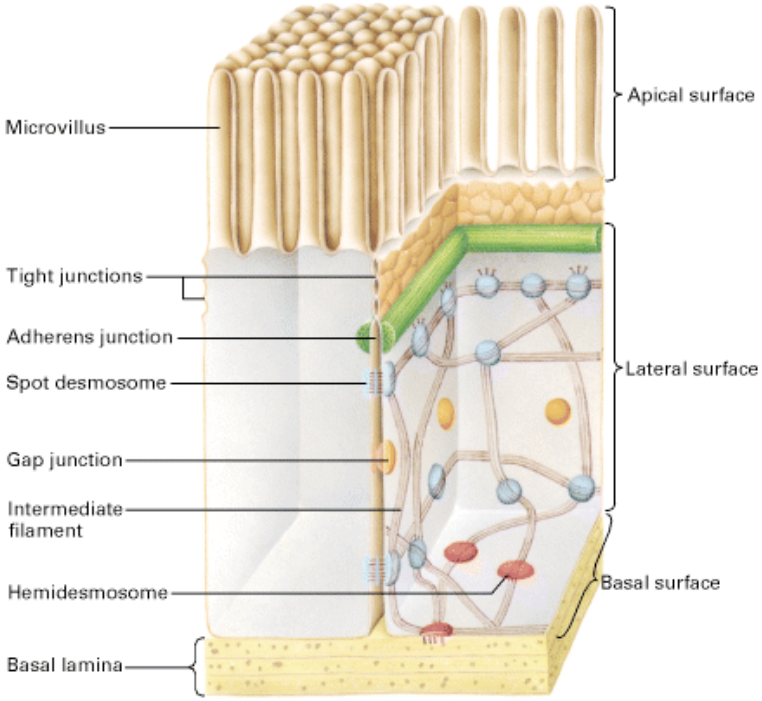

Fig. 3.1.10. Schematic showing the different types of cell junctions present in an epithelial cell as found in the small intestine. Tight junctions near the apical surface essentially prevent the passage of all molecules. The spot desmosomes and adherens junctions provide for cell-cell anchoring, and the hemidesmosomes for anchoring to the basal lamina. Gap junctions provide a means for communication between neighboring cells. [Reproduced from Lodish et al., Molecular Cell Biology, 2000.]

Junction type	**Function**	**Extracellular or adjacent cell attachment**	**Intracellular attachment**
Adherens	structural, cell-cell or cell-matrix	ECM proteins or cadherins in adjacent cell	actin filaments
Desmosome	structural, cell-cell	cadherin	intermediate filaments
Hemidesmosome	structural, cell-matrix	basal lamina via integrins	intermediate filaments
Focal adhesions	structural, cell-matrix	ECM proteins via integrins	actin filaments
Tight junction	regulate transport between cells and along cell	homophillic binding between the transmembrane proteins occludin or	

	membrane	claudins
Gap junctions	cell-cell communication via ion and small molecule exchange	channels formed by connexin subunits

Table 2. Adhesion complexes.

Focal adhesions. A second means by which cells attach to the extracellular matrix is through focal adhesions. These serve a similar function to the hemidesmosomes, and share a common linkage via integrins to the ECM, but are attached on the intracellular side instead to the actin filaments of the cytoskeleton. Actin filaments converge at the site of focal adhesions forming *stress fibers*, strong actin bundles that attach to the β-subunit of the integrins via adapter proteins such as actinin, vinculin and talin. Focal adhesions are instrumental in cell migration, and for this purpose need to be easily formed and disrupted as the cell moves forward. Release or de-adhesion of cells is often mediated by a class of peptides called *dis-integrins* that competitively bind to the RGD site used by integrins to attach to a variety of matrix molecules.

Tight junctions. Control of transport is generally mediated by tight junctions that form an intricate network of seams between two cells (Fig. 3.1.11). As their name implies, these are the tightest of the cell-cell junctions, and the gaps they leave are often small enough to exclude even the smallest ions and molecules. Formed by homophillic binding between the transmembrane proteins occluding and claudins, tight junctions allow epithelial cells to perform their critical role in transepithelial transport and provide for maintenance of differences in concentration between the apical and basal surfaces of these cells. Since occludins are not capable of forming rigid, structural bonds with the cytoskeleton, they are most often associated in a *junctional complex* with adherens junctions or desmosomes that fulfill the structural needs of attachment.

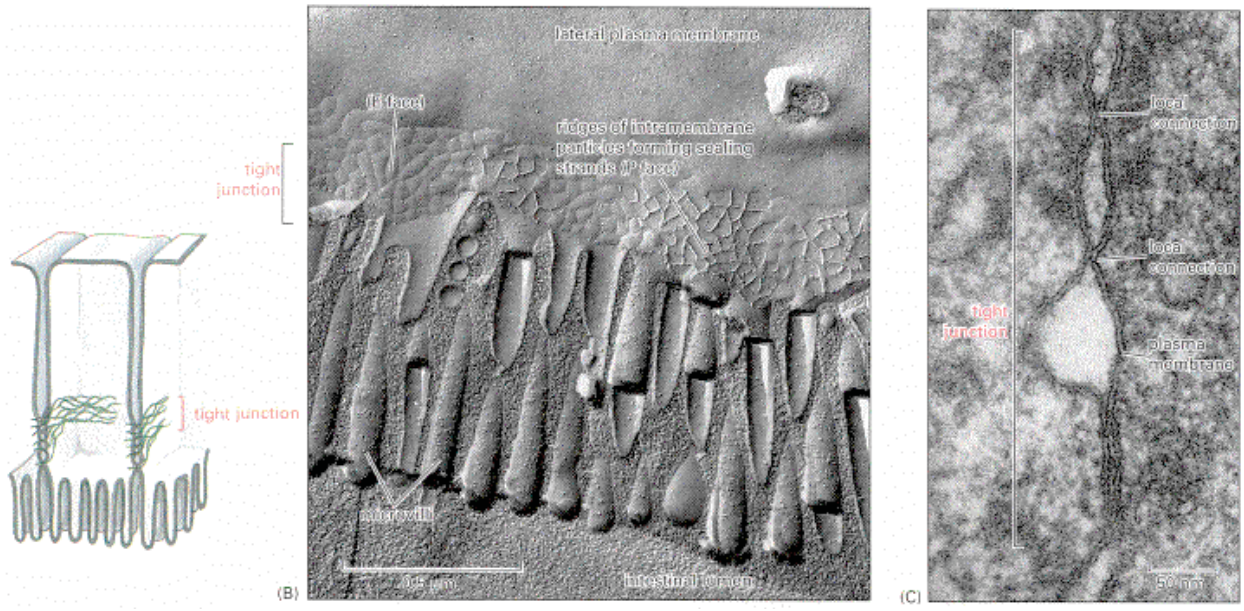

Fig. 3.1.11. Tight junctions in an epithelial cell, shown schematically (a), in a freeze fracture replica (b), and in a transmission electron micrograph (c). [Reproduced from Alberts, et al, 1994.]

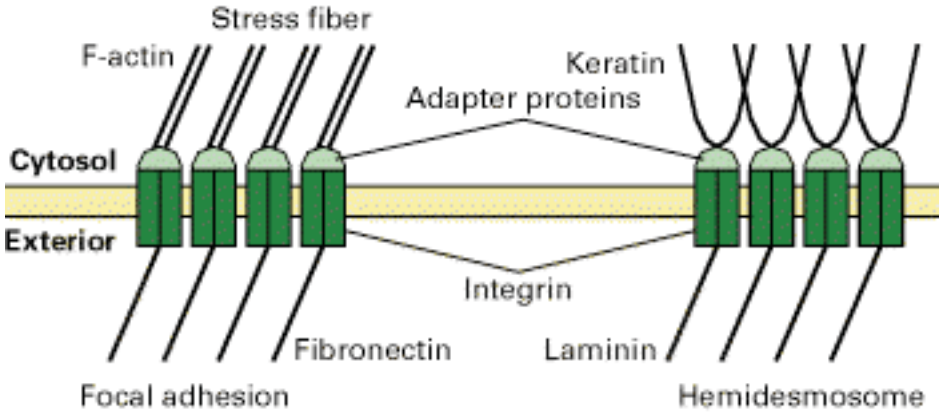

Fig. 3.1.12. Two types of bond that attach a cell to the extracellular matrix by means of clusters of integrins. On the extracellular side, integrins bind to the matrix proteins fibronectin and laminin. Inside the cell, they attach to the cytoskeleton via adaptor proteins to either actin filaments (focal adhesions) or intermediate filaments (hemidesmosomes). [Reproduced from Lodish, et al., Molecular Cell Biolology, 2000]

Non-specific binding.

Cells can adhere to their surroundings by either non-specific or receptor-ligand (specific) bonding. Though both mechanisms are likely active in most situations, as we will see, receptor-

ligand bonding is the stronger of the two, by a considerable margin, and is therefore the most relevant biologically. In situations for which either the receptors or their ligands are not present, however, such as might be the case in certain *in vitro* experiments, non-specific binding can be important as well.

There are essentially three major forms of non-specific attractions to consider:

- *Van der Waals* – These attractive forces arise due to charge interactions in polar molecules. They tend to dominate among the non-specific mechanisms at intermediate distances, around 20-25 nm. [see Boal]
- *Electrostatic* – These interactions can be either attractive or repulsive, depending on the sign of the surface charges, and are particularly important during the approach of two cells since the glycocalyx has a high negative charge density.
- *Steric* – These forces arise due to the steric exclusion of two molecules as they are brought into close contact. In the case of cell-cell interactions, steric repulsion is due to the compression of the two glycocalyx layers and the tendency to resist compression resulting from osmotic effects and the elasticity of the layer. Steric forces tend to dominate for small separation distances < 10 nm.

In combination, these effects combine to produce a net attractive force per unit area of about 100 Pa at a separation distance of about 25 nm.

Adhesion by means of receptor-ligand binding

We can use the analysis of Chapter xx to estimate the strength of a receptor-ligand bond, and based on typical values for bond density, calculate the corresponding strength of adhesion between two cells or between a cell and a surface. Recall that the application of force to a receptor-ligand bond modifies the dissociation rate constant for the binding reaction. This effect can be modeled in several ways, but the result obtained by Bell ((Bell 1978)) suggests the following exponential form for the dissociation rate:

$$k_- = k_-^0 \exp\left(\frac{\gamma f}{k_B T}\right) = k_-^0 \exp\left(\frac{\gamma \sigma}{N_C k_B T}\right) \tag{2.65}$$

where k_-^0 is the unforced dissociation rate constant, γ is a factor with the units of length that corresponds roughly with the distance separating the bonded pair at equilibrium, N_C is the concentration of bonded complex and σ is the average bond force per unit area. To determine

the rate of change of the concentration of bonded pairs, one must solve the following rate equation describing the competition between bond formation (first term) and destruction (second term):

$$\frac{dN_C}{dt} \cong k_+(N_R - N_C)(N_L) - k_- N_C = k_+(N_R - N_C)(N_L) - k_-^0 N_C \exp\left(\frac{\gamma\sigma}{N_C k_B T}\right) \tag{2.66}$$

where N_R and N_L are the concentrations of receptors and ligands, respectively, and we have assumed that $N_C << N_L$, and that *all bonds are stressed equally*. At equilibrium, $dN_C/dt=0$, and if the force applied to detach the cell (equal to the average bond stress, σ) is increased incrementally from zero, N_C will progressively fall to a new equilibrium value. At sufficiently high levels of force, however, increasing σ further eventually gives rise to a situation in which equilibrium can no longer be achieved through a reduction in N_C. At that point, N_C tends toward zero and the cell separates from the surface to which it was attached. It can be shown that this occurs when (Bell 1978)

$$\alpha_c \exp(\alpha_c + 1) = \frac{k_+^0}{k_-^0} N_L \tag{2.67}$$

where $\alpha_c \equiv \frac{\sigma_{\min}\gamma}{N_R k_B T}$ and σ_{min} is the minimum stress needed to cause detachment. For a wide range of conditions, eqn. (2.67) has the approximate solution:

$$\alpha_c \cong 0.7 \ln\left(\frac{k_+^0}{k_-^0} N_L\right) \tag{2.68}$$

so that the critical stress for detachment can be expressed as:

$$\sigma_{\min} \cong 0.7 \frac{N_C k_B T}{\gamma} \ln\left(\frac{k_+^0}{k_-^0} N_L\right) \tag{2.69}$$

where N_C is determined from setting eqn. (2.66) to zero under these critical conditions.

Thermodynamic approach to cell adhesion.

Although we focus here on the mechanical aspects of cell adhesion, this process can also be viewed from a thermodynamic perspective. In this approach, adhesion is considered in terms of the change in energy, specifically the *Gibbs free energy*, G, associated with all the individual receptor-ligand interactions as well as the various non-specific forces of attraction or repulsion. The adhesion of a cell to a given surface, then, can be viewed as an equilibrium state determined

by minimization of the free energy. If, in undergoing a transition from a free state to an adherent state, the system represented by the cell and surface experiences a reduction in free energy, ie, $\Delta G<0$, then adhesion will occur, and the equilibrium state of adhesion will be determined by that with the minimum in free energy, or the largest value of $-\Delta G$. While this approach ignores many of the subtleties of the interactions and, like the analysis above, assumes that all receptor-ligand interactions are identical from an energetic point of view, it is useful in providing some simple insights as seen in the next two examples.

Example: *Comparison of specific and non-specific adhesive forces*: Non-specific bonding due to the combined effects of van der Waals, electrostatic, and steric forces result in an attractive stress of approximately 100 Pa. Receptor-ligand bonding give rise to forces that can be estimated from the change in free energy $f \sim \Delta G/r \sim 9\text{x}10^{-6}$ to $4\text{x}10^{-4}$ dyn/bond = $9\text{x}10^{-11}$ to $4\text{x}10^{-9}$ N/bond where f is the force required to break the bond and r is a measure of the distance the bond stretches before it breaks. Using a typical density of the receptor-ligand complex N_C of $\sim 10^{12}$-10^{15} bonds/m^2 , gives a total bond stress of $N_C \text{ x } f \sim 9 \text{ x } 10^1$ to $4\text{x}10^6$ Pa. The above kinetic approach to estimating bond strength [eqn. (2.69)] gives a value approximately half of that from this equilibrium approach. In either case, however, the conclusion remains the same: non-specific binding can, under certain circumstances, be important since it is comparable to the lowest estimates of receptor-ligand-mediated bond strength, but, not surprisingly, the latter is quite likely to dominate in nearly all practical situations.

Example: *JKR theory for the equilibrium area of adhesion between a cell and substrate*.
It is well known that cells tend to take on a more flattened shape as the substrate to which they are attached becomes more strongly adhesive, either by coating with a more attractive ligand or by increasing the concentration of ligand bound to the substrate. Conversely, less adhesive cells round up and become more spherical. These observations can be explained with the help of a simple scaling analysis, on the assumptions of small deformation of a linear elastic "cell".

Let the cell be modeled as a homogeneous elastic sphere with elastic modulus E and initial radius R (Fig. 3.1.13). It is then brought into contact with a surface to which it adheres. As the cell adheres it attains a lower energy state, characterized by an adhesion energy per unit area J. Formation of a flat adhesion surface, however, requires deformation within the elastic cell and an associated increase in the stored elastic energy. In Chapter 3.1 we showed that the stored elastic energy per unit volume can be written:

$$U_E \approx \int_{V_c} \tau\varepsilon dV \approx \int_{V_c} \tfrac{1}{2} E\varepsilon^2 dV \qquad (2.70)$$

Strain inside the cell can be approximated as the displacement of the cell surface, δ, divided by the characteristic distance within the cell to which the deformations penetrate, a distance that scales with the lateral extent of the contact region, 2*a*, so that $\varepsilon \propto \delta / a$, where it can easily be shown from the geometry that $a^2 \approx 2\delta R$ so that $\varepsilon \propto \sqrt{\delta / R}$. Combining and dropping all numerical constants, we obtain the following scaling approximation:

$$U_E \propto E \frac{\delta}{R} (\delta R)^{3/2} \tag{2.71}$$

An expression for the total energy of the system, then can be written:

$$U \propto -Ja^2 + E\varepsilon^2 a^3 \propto J\delta R + E\delta^{5/2} R^{1/2} \tag{2.72}$$

The equilibrium state corresponds to the value of δ having the minimum energy, obtain from:

$$\frac{\partial U}{\partial \delta} \propto -JR + E\delta^{3/2} R^{1/2} \tag{2.73}$$

so that

$$\delta \propto \left(\frac{JR^{1/2}}{E} \right)^{2/3} \qquad \text{and} \qquad a \propto \left(\frac{JR^2}{E} \right)^{1/3} \tag{2.74}$$

The exact solution to this problem yields the result:

$$a = \left[\frac{9\pi J R^{2(1-\nu^2)}}{2E} \right]^{1/3} \tag{2.75}$$

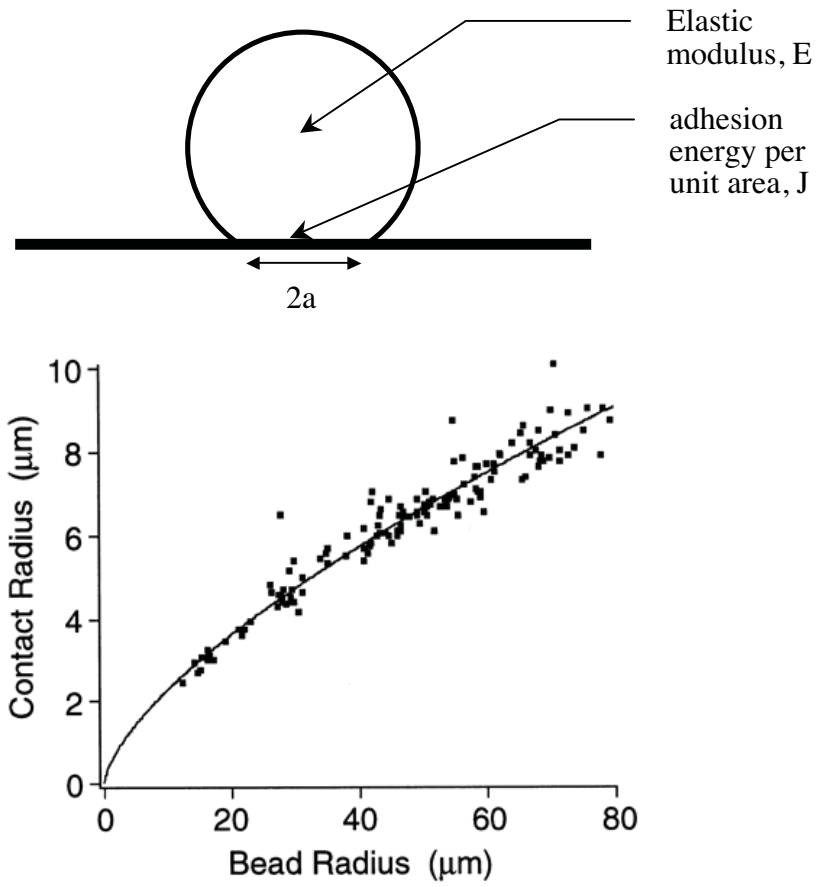

Fig. 3.1.13. Experiments to determine the contact area of an iminobiotin functionalized agarose bead on a glass coverslip in water. Top: Schematic of adherent bead. Bottom: Results for a range of bead radii. Solid line is a fit to the date which obeys the power law, $a \propto R^{2/3}$, consistent with the prediction of JKR theory, eqn.(2.76). [Reproduced from (Moy, Jiao et al. 1999)].

This can be compared to the result obtained from a more rigorous analysis:

$$a = \left[\frac{9\pi J R^2 \left(1 - \nu^2\right)}{2E} \right]^{1/3} \tag{2.76}$$

and to experimental data obtained from spherical beads made from a 4% agarose gel (Fig. 3.1.13).

Models for receptor-mediated adhesion

In Chapter x and in the preceding text we discussed the energetics of bond formation and release, as well as the effect of applied force in altering the energy landscape of the bonded pair and thereby the rate constants for bond kinetics. That analysis has obvious implications to the

adhesion of cells to substrates, the surrounding extracellular matrix, and other cells. Here we extend that analysis in the specific case of whole cell adhesion. In doing so, it will be important to consider such factors as the distribution, type, and density of receptor-ligand bonds or potential bonds, and the elastic properties of the structures to which they are anchored. On the intracellular side, this involves the series of couplings that link the receptor to the cell. In the simplest case, this might simply be a link to the lipid bilayer if the receptor has no intracellular connections. More typically, especially for couplings with a structural role, it involves a series of proteins ultimately linking the receptor to the cytoskeleton.

The typical setting *in vivo* is one in which cells adhere to other cells or to the extracellular matrix. Adhesions are more easily probed, however, through *in vitro* experiments (described below) where cell adhesion more often occurs to an artificial substrate mediated through one of several extracellular proteins that are used to coat the surface. Generally, either collagen or fibronectin is used. Cells are often adhered to these substrates, but to produce a more controlled environment, rigid beads are sometimes coated with the appropriate receptors so that one specific receptor-ligand interaction can be probed. While these systems are useful as models of certain adhesion phenomena, it is important to recognize in the interpretation of these experiments, that when bound to a rigid substrate or bead, the binding proteins cannot freely diffuse, as they would in a more natural environment. In particular, the formation of focal adhesions would not occur in bead-substrate experiments because the receptors would be constrained from aggregating.

It is instructive to begin this discussion with a consideration of a single adhesion bond, for example, one linking the actin matrix of the cytoskeleton to a β_1 integrin, and the integrin receptor binding to the extracellular matrix beyond the cell membrane (Fig. 3.1.14). If the bond is stressed, as for example if the cell experiences a force relative to the ECM, it will at first stretch an amount dictated by the level of force in the bond and the stiffness of the complex. Each bond, as well as each protein in the bond complex, can be thought of as having a certain stiffness, giving rise to a picture in which several springs are considered connected in series. Forces acting on the adhesion complex are transmitted via this series of bonded proteins between the CSK and the ECM, producing local deformations and stresses in the corresponding matrices that decay with distance from the adhesion site. On the intracellular side, these forces are transmitted via a complex involving vinculin, α-actinin, paxillin and talin. Attachment to the extracellular matrix is mediated by an RGD sequence (in fibronectin for example) which in turn, has binding sites for collagen and fibrin. If the force is sufficiently strong, above a certain threshold value F_0 say, and applied for a sufficiently long time, the bond might be severed (de-couple). Typical values of this threshold force lie in the range of 10-100 pN (Evans and Ritchie 1997), but depend, as well, on the rate at which the force is increased. Under more rapid forcings, the threshold is high compared to when the force is increased slowly. This simply

reflects the fact that detachment is a stochastic process and that at any given level of force, there exists a finite probability of detachment, and this probability increases with time.

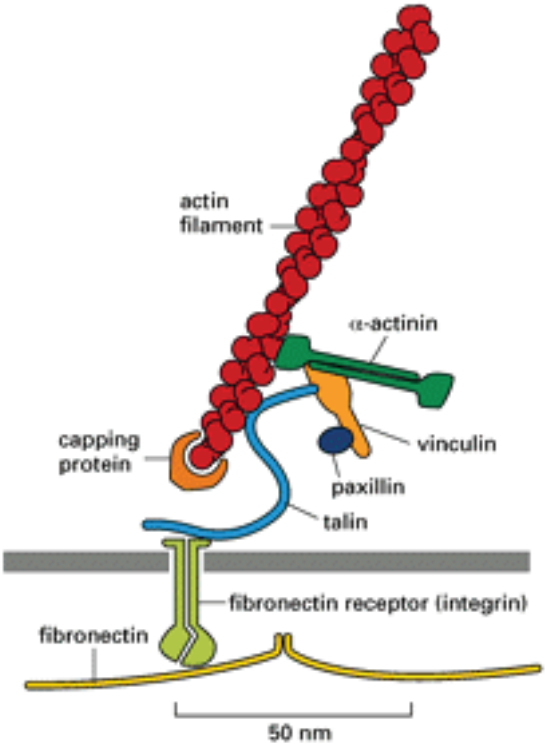

Fig. 3.1.14. One type of attachment linking the intracellular actin matrix to the extracellular matrix via an integrin complex that involves, in addition, vinculin, α-actinin, paxillin and talin. (Reproduced from Lodish, et al., Molecular Cell Biolology, 2000).

We need also to consider that, in equilibrium, a fraction $\Phi = K(1+K)^{-1}$ (where K is the equilibrium constant) of the receptors will be bound at any given time, and that the receptor-ligand complexes are continually cycling between the bound and unbound states, characterized by their respective rate constants.

On a larger scale, numerous adhesion sites typically act in parallel, each contributing some amount to the total adhesion force. If the force transmitted by each single adhesion complex is F, and the density of adhesion sites (per unit membrane area) is N_C, then the *stress* acting on the cell is the product $F\,N_C$. This gives a somewhat false impression, however, as it is unlikely that each adhesion complex carries an equal force. Put another way, there exists a local stress, τ, that can be thought of as the product of the average force per bond times the bond density. This stress is typically non-uniform. In the adhesion of a cell to a flat substrate, the bonds near the periphery of the contact zone determine the strength of the cell against detachment, and when the cell is subjected to a detaching force, the stresses are concentrated in

this peripheral region as depicted in Fig. 3.1.15. In the vicinity of the edge of adhesion, several factors will influence the stress distribution including the mechanical properties of the membrane (in particular the bending stiffness, K_B), the receptor density, the spring constants of the bond, and the bond strength.

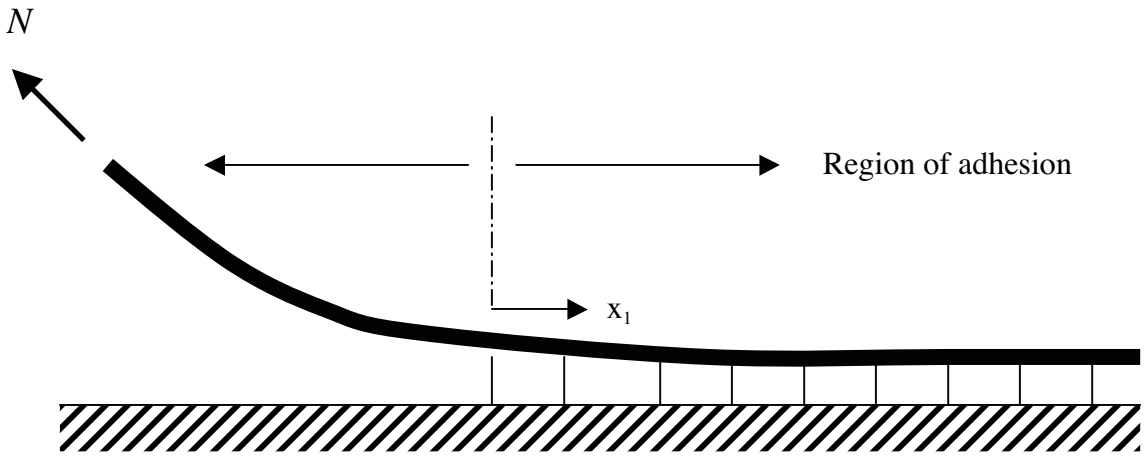

Fig. 3.1.15. Schematic model of a cell membrane being detached from a substrate by application of a tension force N. The membrane is free to the left of the dash-dot line, and adherent to the right. Forces and moments are transmitted through the membrane which adheres to the membrane through receptor-ligand bonds represented by a continuous distrubution $p(x_1)$.

To illustrate, consider the following simple model for an adherent cell being peeled away from its substrate by a force that generates a tension, N, in the membrane (Fig. 3.1.15). Deformations in the membrane are described by eqn. (2.23) where it can be shown that the bending term dominates provided $K_b/L^2 > N$ where L is the characteristic length in the x_1 direction (due to the small length scales involved), and the external membrane force (p in the membrane equation), is now the non-uniform stress due to adhesion bonds. As a simple first approximation, we take $p = k(\delta - \delta_0)$ with $\delta - \delta_0$ being the amount of stretch in the receptor-ligand bond "springs" and k an effective bond spring constant. Recognizing that p approaches zero far from the edge (see Fig. 3.1.9), the membrane displacement and the spring displacement are related: $u_3 = \delta - \delta_0$. Thus, eqn (2.28) is written:

$$K_B\left(\frac{\partial^4 u_3}{\partial x_1^4}\right) = N_C F = N_C k u_3 \tag{2.77}$$

This can be solved directly showing that the distance of separation between the cell membrane and substrate grows in an exponential fashion with distance. Even more simply, a scaling

analysis of eqn. (2.77) in which the term on the left is approximated by $K_b u_3/w^4$ where w is the characteristic distance over which u_3 varies, tells us that the stresses are concentrated in a region of width

$$w \propto \sqrt[4]{\frac{K_B}{N_C k}} \tag{2.78}$$

near the cell periphery. Similarly, we can estimate that the cell membrane will detach from the substrate if $N > F_o N_C w$, where F_0 is a measure of the force in a single bond at the time of bond rupture, and that the rate of peeling can be roughly approximated as the product of the disassociation rate, k_- (bonds/s) from eqn. (2.65) and the distance between bonds ($N_C^{-1/2}$). Although this provides some insight into how the peeling rate depends on the various factors, it fails to capture the fact that the cell remains in an equilibrium attached state even for non-zero levels of tension, reflecting that even under force, a balance can exist between the rates of formation and rupture of receptor-ligand complexes. (Ra, Picart et al. 1999)

It is also of interest to note that, in the region near the edge of the attachment zone(x_1=0 in Fig. 3.1.15), the membrane acts as a beam subjected to a moment due to the applied tension. This moment is balanced by a force couple due to tension in the adhesion complexes right adjacent to the edge in combination with a compressive stress between the cell and substrate a little further in. In typical situations, this compressive stress can approach levels as high as one atmosphere, and can act to effectively smooth the membrane and recruit new attachment sights.

While using these continuum descriptions, it is important to keep in mind the true, discrete nature of the individual bonds represented in the model as a continuous adhesive surface. This is brought to light by a simple calculation in which the characteristic length over which the applied tension is supported, w, is compared to the inter-receptor spacing, $N_C^{-1/2}$. Using typical values for the parameters: $N_C = 10^3$ complexes·μm^{-2}, $k = 10^{-5}$ to 10^{-6} N/m, $K_b = 1$ to $2\text{x}10^{-18}$ Nm, we find that $w \cong 0.1$ to 0.3 μm and the inter-complex spacing, $N_C^{-1/2} \cong 0.03$ μm. While it is reassuring to see that w is typically less than the inter-complex spacing, the difference is small. It is therefore not surprising that the actual process of cell peeling is stochastic in nature, occurring in a sequence of more-or-less discrete steps with a velocity of peeling that varies widely from the mean.

The interplay between receptor-ligand bonding and membrane stiffness also determines whether a cell will spread over a surface or peel away from it under a given tension. Membrane bending stiffness acts to maintain the membrane and substrate within close proximity near the edge of contact (Fig. 3.1.15). Spreading can occur, only if their separation distance is within the extended length of the receptor ligand bond over a distance comparable to the linear spacing

between neighboring bonds ($N_C^{-1/2}$). Under high tension, the surfaces rapidly diverge and spreading is prevented; if the tension is sufficiently low, receptor-ligand bonding can occur and spreading can occur.

Measurements of adhesion

A variety of methods have been used to experimentally determine the strength of adhesion, either of individual receptor-ligand bonds or populations of bonds, as in the case of entire cells. Whole cell experiments are more common, and typically require less experimental sophistication. The drawback, of course, is that they provide only for estimates of average properties and require certain assumptions regarding the distribution of cell-substrate adhesive stress for interpretation to the level of a single bond. Several of these methods are described next.

Centrifugal cell adhesion assays. In this experiment, cells are allowed to attached to a substrate, then are placed in a centrifuge rotating at speed, ω, positioned a distance r from the center of rotation and oriented so that the net centrifugal force is acting to separate the cell from the substrate. Using the arrangement shown in Fig. 3.1.16 (right), the acceleration of the cells is $\omega^2 r$, and the net force acting on a cell of volume V_c is $F = \left(\rho_c - \rho_f\right)\omega^2 r V_c$ where the fluid and cell densities are ρ_f and ρ_c, respectively.

Interpreting these results, we can make several different assumptions each leading to a different estimate for the maximum force experienced by the binding complex. If we simply assume that all receptor-ligand complexes support an *equal* fraction of the total force, F, then the force per bond is $f = F/\left(\pi a^2 N_C\right)$ where N_C is the concentration of bond complexes. However, as the cell tears away from the substrate, the edge bonds will break first, since these experience the greatest level of force. An alternative approach, then, is to assume that the adhesion complexes around the cell circumference support the entire load, leading to the estimate $f = F/\left(2\pi a N_C^{1/2}\right)$, recognizing that $N_C^{1/2}$ is the average distance between bonds. A somewhat more accurate value for f might be obtained if we assume that all complexes within the distance w given by eqn. (2.78), support the load. In any of these cases, once the centrifugal force exceeds some critical limit, since the number of receptors supporting the load falls as the region of contact becomes smaller, the force per bond increases and the cell will rapidly detach.

Stochastic variability also needs to be taken into account, however, since even under a constant load, any single bond has a finite probability of failure under a given level of force. The equilibrium state of the cell, then, should be viewed as one in which the rate of bond formation equals the rate of bond breakage, with increasing force having the effect of reducing the

probability that the bond will remain intact. These effects can be addressed using the methods described in more detail in Chapter xx.

Parallel flow assay. Another common method for assessing cell adhesion is to plate the cells onto one wall of a parallel flow chamber, subject them to a fluid dynamic shear stress and observe at what flow rate the cells begin to release. If we ignore flow details in the immediate vicinity of the cell, the shear stress can be estimated from the solution for a fully developed (Poiseuille) velocity profile:

$$v(y) = \frac{3\bar{V}}{2}\left[1 - \left(\frac{y}{h}\right)^2\right] \tag{2.79}$$

so that the shear stress acting on the cell is

$$\tau_w = \mu\left(\frac{dv}{dy}\right)_{y=-h} = \frac{6\mu\bar{V}}{h} \tag{2.80}$$

and the total force can be estimated as $F \approx \tau_w A_c$ where A_c is the surface area of the cell membrane exposed to the flow.

Consider, as an example, a flow of culture medium at a rate of 1 ml/s through a channel of height 0.1 cm and width 1 cm. If the culture medium has a viscosity close to that of water, (μ=0.01 dyn·s), the shear stress is obtained from eqn. (2.80):

$$\tau_w = \frac{6\cdot(0.01 dyn\cdot s)\cdot(1 ml/s)/(0.1\cdot 1.0 cm^2)}{0.1 cm} = 6 dyn/cm^2 = 0.6 Pa$$

This corresponds roughly with the level of shear stress experience by endothelial cells in the arterial system. If we consider that the cell has a surface area with dimensions roughly 100 μm x 10 μm or about 10^3 μm^2, then the total force acting on the cell is obtained by integrating the shear stress over the area of the apical membrane. Assuming that the shear stress is uniform, the force is simply the product of shear stress and surface area, or about 1 nN in the present example.

Again, interpretation of results from such experiments requires careful consideration of the distribution of forces among the individual adhesion complexes. In this situation, the cell is likely to peel from the upstream edge, in much the same manner as occurs in the cell peeling experiment discussed earlier.

Radial flow and spinning disk assays. One disadvantage of the parallel flow assay is that all cells are subjected to essentially the same level of shear stress, so the flow rate needs to be incrementally varied in order to determine the level of force required for detachment. These two systems using an axisymmetric geometry circumvent this problem by producing an easily characterized radial variation in shear stress. In the case of the *radial flow assay*, fluid enters through a central channel and flows radially outward through the narrow gap between two circular plates. From conservation of mass, the mean flow velocity is given by

$$\bar{V} = \frac{Q}{2\pi r h} \tag{2.81}$$

and sufficiently far from the center ($r>>h$), the velocity profile is parabolic as in the parallel flow assay, and the shear stress is again governed by eqn. (2.80) using (2.81) for $\bar{V}$.

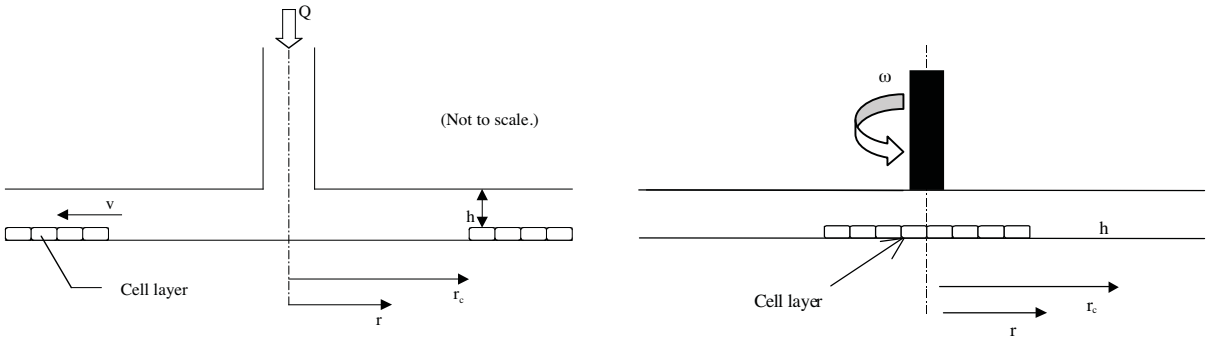

Fig. 3.1.16. Schematic diagram showing the radial flow assay (left) and the spinning disk assay (right). In the radial flow assay, shear stress attains a maximum value near the center and falls with increasing radius r, whereas in the spinning disk system, maximum shear stress is experienced at large r.

In the *spinning disk assay*, cells are grown on one disk, and the opposite disk is rotated at constant speed. Provided the rate of rotation is sufficiently small that inertial effects can be neglected, the velocity is purely in the circumferential direction and the profile is linear between the two plates, so that the shear stress experienced by the cells can easily be computed as

$$\tau_w = \mu \frac{\omega r}{h} \tag{2.82}$$

In both of these cases, as in the parallel flow assay, the total force is obtained by integrating the shear stress over the cell surface, and the distribution of force among the adhesion complexes is weighted toward those located near the upstream end of the cell. This can also be seen by consideration of the torque exerted by shear stress on the cell that must be balanced by a non-uniform contact stress with the substrate that is greatest near the upstream end.

Single bond adhesion assays. Two other assays provide a means of obtaining estimates for the strength of a single adhesion bond without the need for excessive interpretation. These rely on an ability to isolate a small number of bonds, or even a single bond, and infer bond strength from the step-wise nature of the de-adhesion process associated with breakage of discrete bonds. One of these methods employs the atomic force microscope, coated with the ligand of an adhesion receptor, as shown in Fig. 3.1.17. The probe tip is gradually brought up to the cell surface until one or more receptor-ligand bonds are formed. When the probe tip is withdrawn, it moves along a different trajectory on a force-displacement plot, reflecting the forces of adhesion. These forces are seen to jump between more or less discrete levels as the probe continues to be moved away from the cell, with each jump corresponding to the breakage of a single bond (Fig. 3.1.17). Using this method, the bond strength between integrin receptor and a variety of RGD-containing ligands was found to lie in the range of 30 to 100 pN (Lehenkari and Horton 1999).

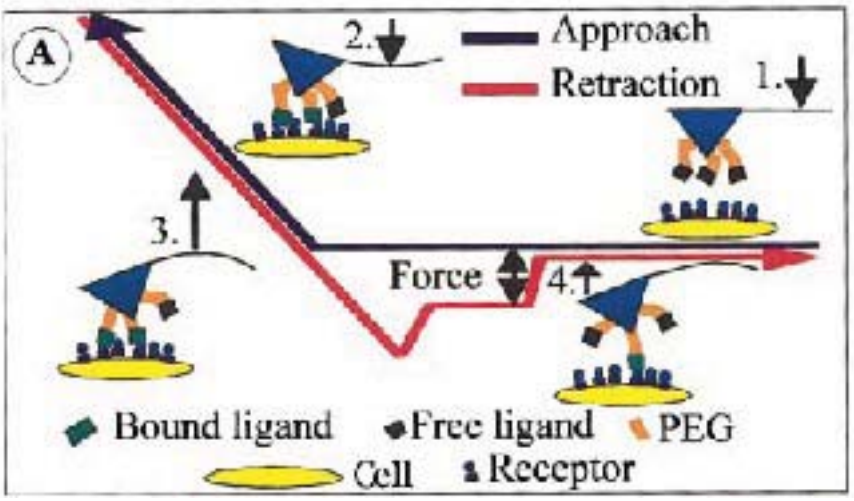

Fig. 3.1.17. The strength of a single adhesion bond can be measured by bringing a functionalized tip of an AFM probe up to the cell, allowing bonds to form, then slowly withdrawing the probe. Monitoring the differences between the force displacement curve between the forward and reverse motions, the forces necessary to break a single receptor-ligand bond can be determined. [Reproduced from (Lehenkari and Horton 1999).]

A second method is similar in that the discrete increments in force are monitored as individual receptor-ligand bonds are broken, but the forces are measured by means of changes in the shape of a giant vesicle the membrane of which contains the ligands have been inserted. In this case, one vesicle is made effectively rigid due, for example, to a high surface tension. A second vesicle containing the adhesion molecules is also drawn partially into a micropipet, but is much more complaint than the first. The two vesicles are then brought into point contact so that one or a small number of adhesions are formed. As the pipets are moved apart, the compliant vesicle distorts due to the force of adhesion which, it can be shown, is related to the change in dimension of the vesicle in the direction of the force, thereby serving as a sensitive force transducer, measuring forces in the range of single adhesion receptors, or between 1 and 100 pN [Evans, 1991 #37].

(For specific examples of leukocyte rolling and attachment see Orsello, or Chang & Hammer)

[This process is initiated, for example, by local infection that causes the release of chemotactic agents in addition to cytokines ….

Models of this process draw upon many of the concepts discussed in this chapter.]

Transient cell adhesion.

Concepts of transient adhesion and release are of particular importance in the case of leukocyte rolling, adhesion and transmigration across the endothelial layer of a blood vessel. In addition, cell migration through extracellular matrix or along a substrate requires the ability of the cell to both form and release adhesions.

One problem that has received considerable attention is the interaction between an adherent or rolling leukocyte and the adhesion receptors on the endothelium. These studies are complicated by the three-dimensional nature of the flow, the compliance of the interacting surfaces, and receptor-ligand dynamics. In a series of recent studies, Hammer and co-workers (Chang, Tees et al. 2000) have addressed several of these issues, computing the viscous force and torque acting upon a sphere near to planar wall from the mobility matrix (Hammer and Apte 1992) and using the "Bell model" of receptor binding (Bell 1978), but neglecting the effects of cell deformation. The Bell model relates the dissociation rate constant, k_r to the force in the bond, f, the thermal energy, $k_B T$, and a parameter with units of length that depends on the reactivity of the molecule:

$$k_r = k_r^o \exp(\gamma f / k_B T) \tag{2.83}$$

A Monte Carlo method is employed at each time step in the calculation to determine bond formation or breakage. In these studies, the nature of the leukocyte-endothelial interaction is characterized as firm adhesion, rolling adhesion, bimodal adhesion, or no adhesion, and mapped as a function of the two parameters of the Bell model in Fig. 3. The boundaries of the rolling adhesion regime are identified for a wall shear rate of 100 s^{-1} (dotted lines) or 30 and 400 s^{-1} (solid lines). Most literature values for the Bell model parameters for a variety of selectin receptors (known to be instrumental in leukocyte rolling) correspond to the rolling adhesion regime for typical shear rate of 100 s^{-1}. An interesting, but counterintuitive result from this study was the observation that, as the bond stiffness was increased from the value used in most calculations (100 dyne cm^{-1}), adhesiveness *decreased*, which the authors attribute to reduced deflection for a given level of force, leading subsequently to more rapid dissociation.

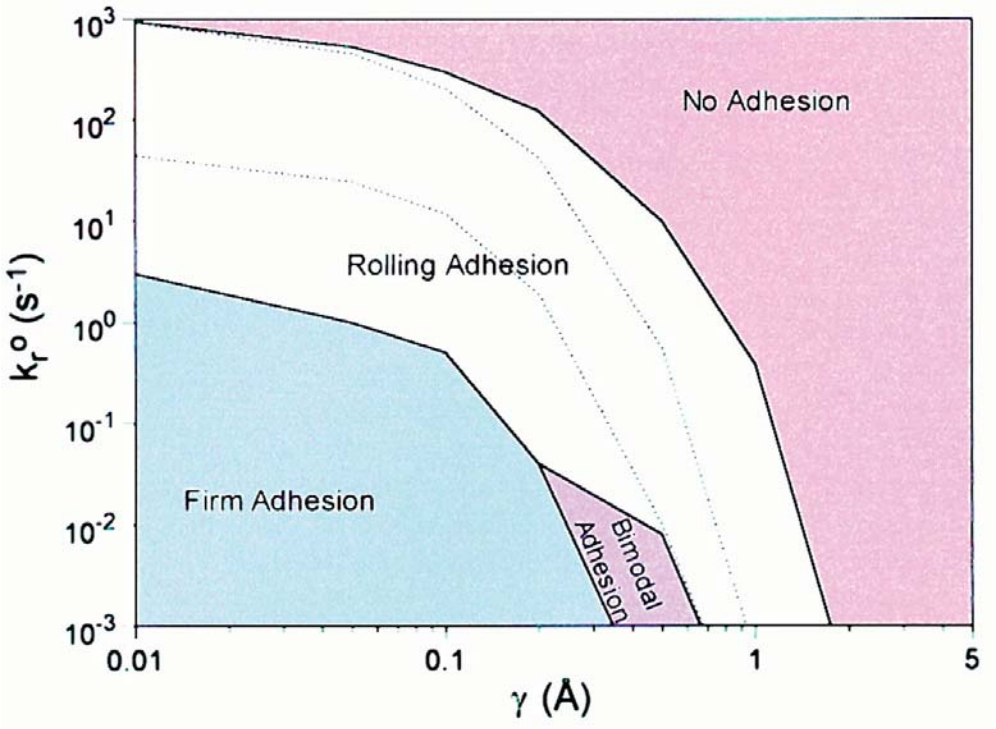

Fig. 3.1.18. The state diagram for a leukocyte interacting with an endothelial surface for shear rates ranging from 30 to 400 s^{-1}. For low dissociation rates, the leukocyte remains adherent to the surface (lower left). As either (γ) or (k_r^o) [see Eqn. (2.83) for definitions] is increased, the cell first adheres firmly, then rolls along the wall, then completely detaches (upper right). Rolling adhesion is defined as the regime where rolling occurs over some part of the shear rate range between 30 and 400 s^{-1}. Firm adhesion indicates that cells remain attached even at the highest shear rate; no adhesion indicates that cells roll at a velocity > 50% of the velocity of a non-adherent sphere. In the bimodal regime cells are either adherent or non-adherent and do not exhibit rolling. Dotted curves correspond to these same boundaries for a shear rate of 100 s^{-1}. Reproduced from Chang et al (2000).

In another recent study using high-resolution video-microscopy (Schmidtke and Diamond 2000), it was demonstrated that a flowing neutrophil can attach to an adherent platelet via adhesion molecules located in the tips of the microvilli and form long tethers averaging nearly 10 μm in length but ranging up to 40 μm at extensional rates of 6-40 μm s^{-1} for shear rates ranging from 100-250 s^{-1}. The mechanics of tether formation is itself a fascinating topic that is still under intense investigation. Readers interested in pursuing this work in more detail are referred to the several papers (Hochmuth, Shao et al. 1996; Dai and Sheetz 1998; Dai and Sheetz 1999) that identify a number of intriguing phenomena.

3.1.7 **Nomenclature**:

Parameter		Definition	Units
R	-	receptor	
L	-	ligand	
C	-	receptor-ligand complex	
G	-	Gibbs free energy	$N \cdot m$
N	-	membrane tension	N/m
N_R	-	total receptor density	μm^{-2} in 2D or μm^{-3} in 3D
N_L	-	total ligand density	μm^{-2} in 2D or μm^{-3} in 3D
N_C	-	complex density	μm^{-2} in 2D or μm^{-3} in 3D
N_{Rf}	-	free receptor density	μm^{-2} in 2D or μm^{-3} in 3D
N_{Lf}	-	free ligand density	μm^{-2} in 2D or μm^{-3} in 3D
d_+	-	forward diffusional rate constant	$\mu m^2 \cdot s^{-1}$ in 2D or $\mu m^3 \cdot s^{-1}$ in 3D
d_-	-	reverse diffusional rate constant	s^{-1}
r_+	-	forward reaction rate constant	s^{-1}
r_-	-	reverse reaction rate constant	s^{-1}
D_m	-	membrane diffusion coefficient	$\mu m^2 \cdot s^{-1}$
D_s	-	solution diffusion coefficient	$\mu m^2 \cdot s^{-1}$
K_b	-	bending stiffness	$N \cdot m$
K^0	-	equilibrium constant or affinity (zero force) $= k_+^0 / k_-^0$	M^{-1} in 3D and μm^2 in 2D
K	-	equilibrium constant $= k_+/k_-$	M^{-1} in 3D and μm^2 in 2D
k_+^0	-	association rate constant (zero force)	$M^{-1}s^{-1}$ in 3D or $\mu m^{-2} \cdot s^{-1}$ in 2D
k_-^0	-	dissociation rate constant (zero force)	s^{-1}
k_+	-	association rate constant	$M^{-1}s^{-1}$ in 3D or $\mu m^{-2} \cdot s^{-1}$ in 2D
k_-	-	dissociation rate constant	s^{-1}
f	-	force per bond	N
F	-	total adhesion force	N
γ	-	empirical parameter	μm
r_0	-	distance over which energy minimum acts	μm
E_0	-	bond energy	J
k_B	-	Boltzmann's constant	JK^{-1}
T	-	temperature	K
τ	-	bond lifetime	s

τ_0	-	bond lifetime with zero force	s
σ	-	adhesion stress	N μm^{-2}
κ	-	spring constant for receptor-ligand bond	N μm^{-1}

References

Bell, G. I. (1978). "Models for the specific adhesion of cells to cells." Science **200**: 618-627.
Caille, N., O. Thoumine, et al. (2002). "Contribution of the nucleus to the mechanical properties of endothelial cells." J Biomech **35**(2): 177-87.
Chang, K. C., D. F. Tees, et al. (2000). "The state diagram for cell adhesion under flow: leukocyte rolling and firm adhesion." Proc Natl Acad Sci U S A **97**(21): 11262-7.
Dai, J. and M. P. Sheetz (1998). "Cell membrane mechanics." Methods Cell Biol **55**: 157-71.
Dai, J. and M. P. Sheetz (1999). "Membrane tether formation from blebbing cells." Biophys J **77**(6): 3363-70.
Daily, Elson, et al. (1984). "Determination of the elastic area compressibility modulus of the erythrocyte membrane,." Biophys J **45**(4): 671-682.
Evans, E. and K. Ritchie (1997). "Dynamic strength of molecular adhesion bonds." Biophys J **72**(4): 1541-55.
Evans, E. A. (1983). "Bending elastic modulus of red blood cell membrane derived from buckling instability in micropipet aspiration tests." Biophys J **43**(1): 27-30.
Hammer, D. A. and S. M. Apte (1992). "Simulation of cell rolling and adhesion on surfaces in shear flow: general results and analysis of selectin-mediated neutrophil adhesion." Biophys J **63**(1): 35-57.
Hardt, S. L. (1979). "Rates of diffusion controlled reactions in one, two and three dimensions." Biophysical Chemistry **10**: 239-243.
Hochmuth, F. M., J. Y. Shao, et al. (1996). "Deformation and flow of membrane into tethers extracted from neuronal growth cones." Biophys J **70**(1): 358-69.
Kucik, D. F., E. L. Elson, et al. (1999). "Weak dependence of mobility of membrane protein aggregates on aggregate size supports a viscous model of retardation of diffusion." Biophys J **76**(1 Pt 1): 314-22.
Kusumi, A., Y. Sako, et al. (1993). "Confined lateral diffusion of membrane receptors as studied by single particle tracking (nanovid microscopy). Effects of calcium-induced differentiation in cultured epithelial cells." Biophys J **65**(5): 2021-40.
Lehenkari, P. P. and M. A. Horton (1999). "Single integrin molecule adhesion forces in intact cells measured by atomic force microscopy." Biochem Biophys Res Commun **259**(3): 645-50.
McCloskey, M. and M. M. Poo (1984). "Protein diffusion in cell membranes: some biological implications." Int Rev Cytol **87**: 19-81.
Meleard, P., Gerbeaud, C., Bardusco, N., Mitov, M.D., and Ferdandex-Puente, L. (1998). "Mechanical properties of model membranes studied from shape transformations of giant vesicles." Biochimie **80**: 401-413.
Moy, V. T., Y. Jiao, et al. (1999). "Adhesion energy of receptor-mediated interaction measured by elastic deformation." Biophys J **76**(3): 1632-8.
Ra, H. J., C. Picart, et al. (1999). "Muscle cell peeling from micropatterned collagen: direct probing of focal and molecular properties of matrix adhesion." J Cell Sci **112 (Pt 10)**: 1425-36.
Saffman, P. G. (1976). "Bownian motion in thin sheets of viscous fluid." Journal of Fluid Mechanics **73**: 593-602.
Schmidtke, D. W. and S. L. Diamond (2000). "Direct observation of membrane tethers formed during neutrophil attachment to platelets or P-selectin under physiological flow." J Cell Biol **149**(3): 719-30.
Sheets, E. D., R. Simson, et al. (1995). "New insights into membrane dynamics from the analysis of cell surface interactions by physical methods." Curr Opin Cell Biol **7**(5): 707-14.

Vink, H. and B. R. Duling (1996). "Identification of distinct luminal domains for macromolecules, erythrocytes, and leukocytes within mammalian capillaries." Circ Res **79**(3): 581-9.

Waugh, R. and E. A. Evans (1979). "Thermoelasticity of red blood cell membrane." Biophys J **26**(1): 115-31.

Zeman, K., H. Engelhard, et al. (1990). "Bending undulations and elasticity of the erythrocyte membrane: effects of cell shape and membrane organization." Eur Biophys J **18**(4): 203-19.

Zhelev, D. V., D. Needham, et al. (1994). "Role of the membrane cortex in neutrophil deformation in small pipets." Biophys J **67**(2): 696-705.

20.310J / 3.053J / 6.024J / 2.797J Molecular, Cellular, and Tissue Biomechanics
Spring 2015